

AD-A215 189

2

DTIC FILE COPY

R89-917259-2

# Study of Adherent Oxide Scales

Contract No. N00014-85-C-0421

DTIC  
ELECTE  
DEC 05 1989  
S D CG D

J. G. Smeggil  
United Technologies Research Center  
East Hartford, Connecticut

October 27, 1989



DISTRIBUTION STATEMENT A  
Approved for public release;  
Distribution Unlimited

89 11 22 019

REPORT DOCUMENTATION PAGE				Form Approved OMB No. 0704-0188	
1a. REPORT SECURITY CLASSIFICATION Unclassified			1b. RESTRICTIVE MARKINGS		
2a. SECURITY CLASSIFICATION AUTHORITY			3. DISTRIBUTION / AVAILABILITY OF REPORT		
2b. DECLASSIFICATION / DOWNGRADING SCHEDULE					
4. PERFORMING ORGANIZATION REPORT NUMBER(S)			5. MONITORING ORGANIZATION REPORT NUMBER(S)		
6a. NAME OF PERFORMING ORGANIZATION United Technologies Research Center		6b. OFFICE SYMBOL (If applicable)	7a. NAME OF MONITORING ORGANIZATION		
6c. ADDRESS (City, State, and ZIP Code) Silver Lane East Hartford, CT 06108			7b. ADDRESS (City, State, and ZIP Code)		
8a. NAME OF FUNDING / SPONSORING ORGANIZATION Office of Naval Research		8b. OFFICE SYMBOL (If applicable)	9. PROCUREMENT INSTRUMENT IDENTIFICATION NUMBER		
8c. ADDRESS (City, State, and ZIP Code) Department of the Navy Arlington, VA 22217			10. SOURCE OF FUNDING NUMBERS		
			PROGRAM ELEMENT NO.	PROJECT NO.	TASK NO.
11. TITLE (Include Security Classification)  Study of Adherent Oxide Scales					
12. PERSONAL AUTHOR(S) John G. Smeggil					
13a. TYPE OF REPORT Final Report		13b. TIME COVERED FROM 1/1/89 TO 9/30/89		14. DATE OF REPORT (Year, Month, Day)	
15. PAGE COUNT					
16. SUPPLEMENTARY NOTATION					
17. COSATI CODES			18. SUBJECT TERMS (Continue on reverse if necessary and identify by block number)		
FIELD	GROUP	SUB-GROUP	>Oxidation, Oxide Scale Adherent, Oxide Scale formation, minor element effect, Sulfur, (PROTECTIVE CHROMIUM OXIDES)		
19. ABSTRACT (Continue on reverse if necessary and identify by block number)  Previously reported studies had shown that indigenous sulfur normally present in the approximately 1-40 ppm range significantly affected the scale adherence of both alumina and chromia formers. In isothermal studies involving the oxidation of the model chromia former, Ni-40 wt. % Cr, visual examination of alumina crucibles containing test specimens and subsequent analytical chemistry measurements showed that protective chromium oxides exhibited less volatility on high purity as compared to normal sulfur-containing alloys. While the absolute amount of chromium evaporated was small, higher purity (lower sulfur) alloys repeatedly showed less chromia volatilization. For cyclic tests involving sulfur-bearing (SO <sub>2</sub> -O <sub>2</sub> ) environments, sulfur penetration of chromia scales occurred regardless of the purity of the alloy or whether or not yttrium had been added to the normal purity alloy. However, for the normal purity alloys Ni-40 wt. % Cr and Ni-40 wt. % Cr-0.5 wt. % Y substantially more internal and grain boundary oxidation had occurred than for the high purity alloy. Experiments were conducted to determine whether chromium additions to stoichiometric (Ni-30 wt. % Al) and hypostoichiometric (Ni-25 wt. % Al) NiAl could					
20. DISTRIBUTION / AVAILABILITY OF ABSTRACT <input type="checkbox"/> UNCLASSIFIED/UNLIMITED <input type="checkbox"/> SAME AS RPT. <input type="checkbox"/> DTIC USERS			21. ABSTRACT SECURITY CLASSIFICATION		
22a. NAME OF RESPONSIBLE INDIVIDUAL			22b. TELEPHONE (Include Area Code)		22c. OFFICE SYMBOL

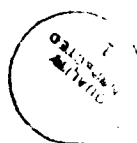
19. Cont.

substitute for yttrium additions thereby producing oxide scale adherence. Chromium additions (from 1 to 7 wt. %) did not have the beneficial effects desired. In fact, chromium additions generally debited the oxide scale adherence in comparison to behavior observed for the base line alloys.

*Study of Adherent Oxide Scales*

TABLE OF CONTENTS

	Page
I. INTRODUCTION .....	I-1
II. EXPERIMENTAL PROCEDURES AND MATERIALS .....	II-1
III. EXPERIMENTAL RESULTS .....	III-1
1. The effect of indigenous sulfur on the evaporation of thermally grown chromia scales. ....	III-1
2. Effect of SO <sub>2</sub> on the 1000°C cyclic oxidation behavior of normal and high purity Ni-40 wt. % Cr. ....	III-1
3. Attempts to determine if chromium additions could replace yttrium additions in inducing a "reactive element" effect in approximately stoichiometric and aluminum-deficient (hypostoichiometric) NiAl. ....	III-2
IV. DISCUSSION .....	IV-1
V. SUMMARY AND CONCLUDING REMARKS .....	V-1
VI. REFERENCES .....	VI-1



per CS

A-1

## *Study of Adherent Oxide Scales*

### I. INTRODUCTION

In the presence of ambient environments at elevated temperatures, all structural alloys are thermodynamically unstable reacting to form oxide scales. In order for such thermally grown oxide scales to be protective, they must limit the reaction rate between atmospheric oxygen and the substrate alloy. Oxidation rates are limited by scales which exhibit the following properties: (1) slow growth kinetics; (2) minimal vaporization effects at temperatures of interest; (3) minimal interaction with molten salts which might be present on hardware surfaces and (4) adherence under thermal cycling conditions.

For the majority of alloys which form either alumina or chromia scales, the latter property—oxide scale adherence under thermal cycling conditions—generally controls service life.

To achieve enhanced oxidation resistance, low levels of reactive elements such as yttrium, zirconium, etc. have frequently and repeatedly been documented in the literature to promote beneficial adherence effects. As might be expected with the positive improvements achieved from small additions of reactive elements, numerous studies have been conducted over the years to try to identify the cause of their benefit. Despite extensive studies conducted over many years, there has been no general consensus as to the mechanism responsible for the improvements observed. Several mechanisms reported in the literature to account for behavioral improvements observed include the following:

- (a) the formation of oxide pegs which "anchor" the scale to the substrate (Ref. 1);
- (b) the prevention of vacancy coalescence at the scale-substrate interface by providing for alternative coalescence sites (Ref. 2);
- (c) increased oxide scale plasticity (Ref. 3);
- (d) modification of oxide growth processes (Ref. 4);
- (e) formation of graded scales which would minimize thermo-mechanical differences (Ref. 5); and
- (f) modification of bonding forces through preferential segregation of the active element to the scale-metal interface (Ref. 6).

While the above effects have been suggested to occur for both alumina and chromia scales, only in the case of chromia scales has the formation of mixed oxides been suggested to account for the benefits observed (Ref. 1).

Previous studies conducted at UTRC have indicated that an additional previously unappreciated effect strongly influences the adherence of both alumina and chromia oxide scales (Ref. 7-9). Based on that work, sulfur indigenously present at low levels (approximately 20 to 40 ppm) segregates to the free metal surface at elevated temperature as primarily documented by Auger studies (Ref. 8, 10, 11). With the addition of an active element, the surface segregation of sulfur is markedly reduced (Ref. 8, 12). These findings suggested that for similar experiments conducted in atmospheres and conditions which would promote the formation of an oxide scale similar segregation effects would occur.

However in the presence of a barrier oxide layer, sulfur segregation would be to the critical scale-metal interface rather than to the free metal surface in the high vacuum chamber of an Auger spectroscope. This segregation has been observed by UTRC (Ref. 13) and has subsequently been confirmed by other authors (Ref. 10). UTRC studies have shown based on Auger, ESCA (Electron Spectroscopy for Chemical Analysis) and EDS (Energy Dispersive X-ray Spectroscopy) that for the alumina former Ni-20 wt. % Cr - 12 wt. % Al, the sulfur present at the interface was there as a refractory sulfide as well as a moiety with properties similar to elemental sulfur (Ref. 13).

Using this information as a basis, UTRC conducted experiments which have demonstrated that, by reducing the sulfur content of the alumina-forming alloy Ni-20Cr-12Al alloy, oxide scale adherence was strikingly improved. In the case of both 1050°C and 1180°C cyclic testing, standard purity alloys of Ni-20Cr-12Al typically containing approximately 30-40 ppm sulfur as determined by glow discharge mass spectrometry techniques showed poor oxide scale adherence. By reducing the sulfur content to the approximately 1-2 ppm level, oxide scale adherence was markedly improved effectively equivalent to that produced on alloys with reactive element, i.e. yttrium, additions (Ref. 14).

Those findings relating the adherence of protective alumina scales have been confirmed and substantiated by other experimenters (e.g. Ref. 15).

Extending those studies to chromia formers, experiments were conducted with the model chromia former Ni-40 wt. % Cr (Ref. 5). In that work, experiments were conducted with normal (with regard to sulfur content) purity alloys and high purity (low sulfur) alloys. Normal purity alloys contained indigenous sulfur at levels of approximately 40-57 ppm while the high purity material contained sulfur at a level of 1.45-1.81 ppm.

In cyclic oxidation experiments, little difference was observed for tests conducted at either 900°C or 1100°C (Ref. 9). However in 1000°C cyclic testing, a marked improvement was observed in the oxidation of the low sulfur alloy as opposed to the normal sulfur alloy. Thinner, more adherent oxide scales formed which showed no internal oxidation.

Studies reported here were primarily intended to further characterize the effect of both indigenous and extrinsic sulfur sources on the oxidation behavior of chromia formers. In addition experiments were conducted to determine if chromium itself could substitute for yttrium in additions to hypo- and stoichiometric NiAl.

## II. EXPERIMENTAL PROCEDURES AND MATERIALS

In selecting a typical chromia former, the alloy Ni-40 wt. % Cr was chosen. Alloys of conventional high purity starting materials were prepared by standard vacuum metallurgy techniques. For the conventional standard purity alloys, 99.9 wt. % chromium and 99.99 wt. % nickel were used. Alloys from high purity, i.e. specifically low sulfur level, metals purchased from MRC were prepared by arc melting small (approximately 20 gram) buttons. All prepared ingots or buttons were homogenized in hydrogen for 24 hours at approximately 1200°C prior to sectioning. After metallographic sectioning, specimens were ground to 600 grit SiC prior to oxidation experiments.

Typical analyses of the nominally Ni-40 wt. % Cr alloy materials used here are:

<u>Ingot Designation</u>	<u>Wt. % Chromium*</u>	<u>Sulfur** (ppm by wt.)</u>
Normal purity	40.00 (0.44)	40; 57
High purity	39.59 (0.13)	1.45; 1.81

\* Performed using ICP-AES (Inductively Coupled Plasma - Atomic Emission Spectroscopy). Analyses reported are the average of two determinations with the value in brackets equal to half of the difference between the two determined values.

\*\* Determined by GDMS (Glow Discharge Mass Spectrometry).

To compare and contrast the effect of yttrium and indigenous sulfur, a normal purity Ni-40 wt. % Cr alloy containing a small yttrium addition was used. This alloy contained 40.63 wt. % chromium and 0.55 wt. % yttrium.

To determine if chromium itself could alone provide a "reactive element" effect, the following table lists the nominal alloys examined along with their analyzed compositions.

Aluminum-Rich NiAl Alloys				
<u>Nominal Alloy</u>	<u>Ni</u>	<u>Wt. %*</u>		
		<u>Al</u>	<u>Cr</u>	<u>Y</u>
Ni30Al	67.09 (0.04)	31.50 (1.56)		
Ni30Al1Cr	65.37 (1.08)	30.25 (1.17)	0.97 (0.02)	
Ni30Al3Cr	65.50 (0.16)	28.85 (1.12)	2.99 (0.03)	
Ni30Al5Cr	63.26 (0.16)	29.12 (0.14)	5.16 (0.02)	
Ni30Al7Cr	62.08 (0.12)	29.04 (0.31)	7.14 (0.07)	
Ni30Al0.1Y	70.98 (0.42)	29.07 (0.24)		0.042 (0.001)

## Aluminum-Deficient NiAl Alloys

Nominal Alloy	Wt. %*			
	Ni	Al	Cr	Y
Ni25Al	72.75 (0.74)	24.36 (0.09)		
Ni25Al1Cr	71.32 (0.09)	24.26 (0.22)	0.98 (0.02)	
Ni25Al3Cr	66.90 (1.11)	24.24 (0.37)	2.77 (0.06)	
Ni25Al5Cr	66.59 (0.48)	24.61 (0.02)	4.90 (0.0)	
Ni25Al7Cr	65.01 (0.10)	25.63 (0.63)	6.87 (0.03)	
Ni25Al0.1Y	72.38 (0.20)	25.30 (0.18)		0.05 (0.01)

- \* Performed using ICP-AES (Inductively Coupled Plasma - Atomic Emission Spectroscopy). Analyses reported are the average of two determinations with the value in brackets equal to half of the difference between the two determined values.

Chemistries for the modified NiAl alloys were deliberately chosen to examine a range of chromium activities (concentrations) extending from solid solution levels to levels where alpha-chromium precipitates were observed.

Like the nickel-chromium alloys, the modified NiAl alloys were annealed for at least twenty-four hours in flowing hydrogen at 1200°C. Specimens cut from these ingots were polished down to 600 grit SiC prior to testing.

In cyclic oxidation experiments, specimens were oxidized for 55 minutes at elevated temperature then allowed to cool to ambient laboratory temperatures before reinsertion into the high temperature zone of the furnace. Specimen weight changes were measured after approximately every 20 cycles. In cyclic oxidation testing, the oxidation performance of a given alloy was generally determined by examining the behavior of two specimens of that composition.

Isothermal experiments were conducted to determine the effect of indigenous sulfur on the evaporation of the thermally formed chromium oxide scales. In these experiments, specimens were contained in a small platinum crucible which was placed in the center of a long quartz tube. The tube was deliberately made long enough such that evaporating chromium-rich oxide species would be able to condense onto the cooler parts of the tube extending outside of the furnace. These experiments were conducted in stagnant laboratory air atmospheres. After testing, the amount of chromium deposited on tube walls was determined by wet chemistry techniques.

For experiments involving SO<sub>2</sub>-O<sub>2</sub> atmospheres, a blended gas consisting of 1.0 vol. % SO<sub>2</sub>-O<sub>2</sub> was diluted with oxygen to achieve the desired 0.1 vol. % SO<sub>2</sub> composition. Gas metering was done with calibrated flow meters.

Oxidized specimens were examined by optical metallography, scanning electron microscopy using dispersive x-ray (EDS) techniques and the scanning electron microprobe with wave length dispersive capabilities.

### III. EXPERIMENTAL RESULTS

#### 1. The effect of indigenous sulfur on the evaporation of thermally grown chromia scales.

Specimens of both normal purity and high purity Ni-40 wt. % Cr in separate alumina crucibles were placed into the stagnant atmosphere of a laboratory furnace at 1000°C. After 100 hours of exposure, removal of the crucibles from the furnace revealed the following.

In the case of the normal purity Ni-40 wt. % Cr alloy, a typical greenish-appearing ring coated the bottom of the crucible juxtaposed to where the specimen lay, Fig. 1A. Greenish deposits such as this are typical of the behavior of chromia forming alloys in oxidation and are commonly observed. On the other hand, for the high purity Ni-40 wt. % Cr alloy, the interior surface of the crucible containing it was significantly less discolored by chromium evaporation, Fig. 1B.

In order to quantify this effect, Ni-40 wt. % Cr specimens were separately placed in a platinum crucible and heated within a quartz tube at 1000°C for 240 hours in stagnant laboratory air. Upon removal from the furnace, the amount of chromium deposited on the cool surfaces of the tube was measured. Mass change measurements were also performed before and after testing to give a measure of the effect of indigenous sulfur on the oxidation behavior of the Ni-40 wt. % Cr alloy. The results of these tests are summarized thusly:

<u>Material</u>	<u>Evaporated Chromium (micrograms)</u>	<u>Mass Change/Unit Area (mc/cm<sup>2</sup>)</u>
Normal purity	45, 52	2.93, 3.68
High purity	34, 36	0.78, 1.13

#### 2. Effect of CO<sub>2</sub> on the 1000°C cyclic oxidation behavior of normal and high purity Ni-40 wt. % Cr.

##### a. Thermogravimetric data.

The results of the thermogravimetric experiments for specimens of normal and high purity Ni-40 wt. % Cr as well as Ni-40 wt. % Cr-0.5 wt. % Y are shown in Figs. 2-4, respectively.

Keeping in mind that thermogravimetric data represent in essence net mass changes occurring during the experiment, net mass losses occur for both high purity Ni-40 wt. % Cr and Ni-40 wt. % Cr-0.5 wt. % Y. On the other hand only positive weight changes are found for the normal purity Ni-40 wt. % Cr.

[In the simplest interpretation, these mass changes would only be correlated to oxide scale adherence (or exfoliation) effects. However the metallographic data indicates that this interpretation does not adequately describe the effects which occurred in this experiment.]

### **b. Metallographic observations.**

The cyclically tested specimens were examined by a combination of light and electron optic techniques. The optical metallography and electron microscopy observations of normal purity Ni-40 wt. % Cr are presented in Figs. 5-7. Similar documentation is depicted in Figs. 8 and 9 for the high purity Ni-40 wt. % Cr specimens and in Figs. 10-12 for the Ni-40 wt. % Cr-0.5 wt. % Y specimens, respectively.

Metallographic examination of the as-prepared annealed alloy specimens showed uniform microstructures with at worst only a very few tiny (micron sized) oxide inclusions. This population of oxide inclusions is normal for specimens prepared in the manner employed here.

Concerning the optical metallography of the specimens tested, obvious and significant differences are noted, cf. Figs. 5, 8 and 10. At relatively low magnifications (100X and 200X), both the normal purity Ni-40 wt. % Cr and the Ni-40 wt. % Cr-0.5 wt. % Y alloy show extensive internal and selective grain boundary oxidation effects, Figs. 5 and 10.

On the other hand, the high purity Ni-40 wt. % Cr alloy shows a thin oxide layer with internal oxidation and porosity affecting only the outermost 50 microns of the specimen. Furthermore unlike the normal purity Ni-40 wt. % Cr specimen no evidence for extensive internal oxidation far into the depth of the specimen and no evidence for grain boundary oxidation are found, Fig. 8.

Hence at relatively low magnifications in optical metallography significant differences are observed between the high purity Ni-40 wt. % Cr alloy and the other two materials studied here.

At higher magnifications (500X or greater) in optical metallography, small (approximately micron-sized) particles are observed within about 40 microns of the surface, Fig. 8. Electron microprobe studies using energy dispersive techniques in a point mode and wavelength dispersive techniques in both point and area modes show that these particles contain sulfur, Fig. 9.

For the normal purity Ni-40 wt. % Cr and the Ni-40 wt. % Cr-0.5 wt. % Y alloy, sulfur enriched particles also occur, Figs. 6-7 and 11-12. Moreover the depth of sulfur intrusion in these materials is far greater, at least 150 microns. In the case of the yttrium-containing alloy, sulfur-enrichments were associated with enrichments of yttrium, Figs. 11 and 12. However in the yttrium-containing alloy, many additional sulfur-rich precipitates were observed which were not associated with any detectable yttrium concentrations, Fig. 12.

Hence it is clear that a far greater amount of both internal oxidation and internal sulfide formation has occurred in case of both the normal purity Ni-40 wt. % Cr as well as the Ni-40 wt. % Cr-0.5 wt. % Y alloys.

### **3. Attempts to determine if chromium additions could replace yttrium additions in inducing a "reactive element" effect in approximately stoichiometric and aluminum-deficient (hypostoichiometric) NiAl.**

Cyclic oxidation tests to 1180°C in air environments were conducted for times up to approximately 800 cycles for aluminum-deficient (hypostoichiometric) NiAl and to approximately 700 cycles for essentially stoichiometric NiAl.

Results for the hypostoichiometric alloys are presented in Figs. 13-18. Similarly the results for the stoichiometric alloy are shown in Figs. 19-24.

[It is to be specifically noted that for these modified NiAl alloys metallographic examination of tested specimens indicate an absolute minimal amount of internal oxidation. For these relatively aluminum-rich alloys, this testing scheme would not be expected to produce significant amounts of internal oxidation. Hence weight change behavior for this testing is a true indication of scale adherence effects. This situation contrasts markedly with that indicated earlier for the Ni-40 wt. % Cr alloys discussed earlier.]

For the base line binary alloys Ni-25 wt. % Al and Ni-30 wt. % Al, not unexpectedly oxide scale exfoliation effects are noted, Figs. 13 and 19.

With the nominal addition of a small amount of yttrium (0.1 wt. Y), scale adherence is effected for both Ni-25 wt. % Al and Ni-30 wt. % Al, Figs. 14 and 20.

In additions of chromium at levels of from 1 to 7 wt. % to the base line alloys, adherent scales are not effected for either the nominally stoichiometric Ni-30 wt. % Al or the aluminum-deficient (hypostoichiometric) Ni-25 wt. % Al alloys, cf. Figs. 15-18 and 21-24.

#### IV. DISCUSSION

Previously reported studies showed that in both isothermal and cyclic oxidation testing to 1000°C in air indigenous sulfur markedly effected the performance of the chromia former Ni-40 wt. % Cr (Ref. 9). Thinner and more adherent scales formed on low sulfur-containing alloys. Minimal amounts of internal oxidation were observed. Furthermore yttrium additions to normal purity Ni-40 wt. % Cr alloys did not produce the benefits observed from alloys with lower indigenous sulfur levels.

In stagnant air tests reported here, greenish-colored deposits were noted on alumina crucibles containing normal purity Ni-40 wt. % Cr alloys after extended air exposure at 1000°C, Fig. 1A. Similar alumina crucibles containing high purity (low sulfur) specimens failed to produce a dark green color, Fig. 1B. The dark green coloration is due to evaporated chromium-containing oxides from the thermally produced chromia scales.

Aware that color effects can be produced by very small amounts of material, relatively simple experiments conducted here involving the collection and subsequent analysis of evaporated chromium deposits from oxidizing specimens with similar dimensions indicates that the indigenous sulfur content did effect the evaporation rate of the chromia scales. Normal purity specimens produced deposits of 45 and 52 micrograms of Cr. High purity specimens produced 34 and 36 micrograms of Cr. The difference is small but repeatable based on the experiments conducted here.

Furthermore with regard to these tests, thermogravimetric data from these experiments indicated lower oxidation rates for the high purity alloy specimens, i.e. 0.78 and 1.14 mg/cm<sup>2</sup>, versus 2.93 and 3.68 for the normal purity specimens. This improvement in thermogravimetric performance is similar to that reported previously (Ref. 9).

With regard to 1000°C cyclic oxidation tests in SO<sub>2</sub>-containing environments, i.e. 0.1% SO<sub>2</sub>-O<sub>2</sub>, all the various Ni-40 wt. % Cr specimens showed ingress of sulfur and its precipitation presumably largely as a chromium sulfide. While the effect occurred independently of the purity of the Ni-40 wt. % Cr alloy, the extent to which sulfur ingress occurred was much greater in normal alloys (both Ni-40 wt. % Cr and Ni-40 wt. % Cr-0.5 wt. % Y) than the high purity Ni-40 wt. % Cr alloy. In the latter case, sulfide precipitates are clearly present at least to approximately 150 microns below the scale surface while only about 40 microns of ingress were observed in the former case.

Internal oxidation and preferential grain boundary oxidation phenomena were commonly observed to a great extent in both the normal purity Ni-40 wt. % Cr and the Ni-40 wt. % Cr-0.5 wt. % Y alloys, Figs. 5 and 10. Essentially entire cross sections of these specimens showed internal oxidation effects. Only very limited amounts of internal oxidation were observed in the case of the high purity Ni-40 wt. % Cr alloy. This zone of internal oxidation only extended to a depth of about 50 microns, e.g. Fig. 8.

The internal oxidation effects were clearly due to the high temperature oxidation tests performed here. None of the initially prepared Ni-40 wt. % Cr materials prior to testing showed any significant amounts of internally dispersed particulate oxide.

Hence while not completely stopping the ingress of sulfur into the Ni-40 wt. % Cr substrate, the indigenous sulfur present within the alloy did have a strong effect both on the extent of that ingress. Also the indigenous sulfur content strongly effected the subsequent amount of internal oxidation and the extent of grain boundary oxidation.

Because of the internal and grain boundary oxidation effects, the thermogravimetric data measured for the cyclic experiments cannot be simply interpreted in terms of oxide scale adherence alone.

Cyclic oxidation experiments were conducted with chromium modified alloys based on Ni-30 wt. % Al and Ni-25 wt. % Al. Attempts to determine if chromium additions by themselves could substitute for elements such as yttrium, thereby producing a reactive element effect in these alloys were unsuccessful. Chromium additions examined ranged from one to seven weight percent. Yttrium additions at the 0.1 wt. % level and analyzed in the range of 0.05 wt. % did effect adherent scales. For alloys with this high an aluminum content, internal oxidation effects were largely avoided. Hence cyclic oxidation data did reflect oxide scale adherence effects.

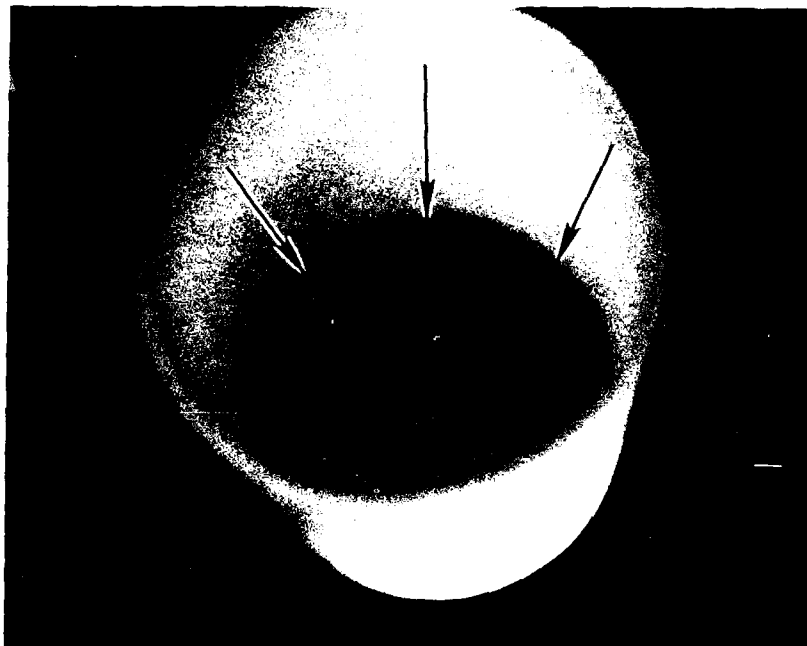
With regard to the chromium-modified NiAl alloys, in general the effect of the chromium addition was to worsen the poor oxide scale adherence shown by the base line alloys, Figs. 13-24.

## V. SUMMARY AND CONCLUDING REMARKS

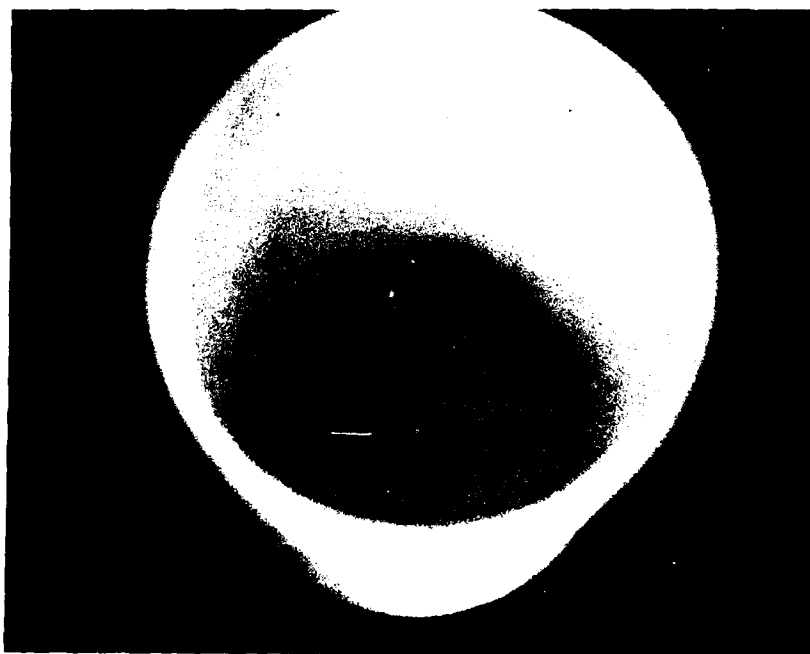
- \* Sulfur is an indigenous element in commonly produced engineering alloys.
- \* Indigenous sulfur at the approximately 30-50 ppm level is sufficient to effect oxide scale adherence and oxidation kinetics. A reduction of the indigenous sulfur results in improved oxide scale adherence and lowered oxidation growth kinetics.
- \* Furthermore at these levels, this indigenous sulfur is associated with a slight reduction in the rate of volatilization of the growing protective chromia scale.
- \* In 1000°C cyclic testing in SO<sub>2</sub> containing atmospheres (0.1% SO<sub>2</sub>-O<sub>2</sub>), sulfur ingress into the Ni-40 wt. % Cr alloy occurs regardless of whether the substrate has normal or reduced sulfur levels. Moreover yttrium additions did not prevent this phenomenon.
- \* However the extent of sulfur ingress is significantly lessened in the case of the alloy with lower indigenous sulfur, i.e. high purity Ni-40 wt. % Cr.
- \* Furthermore in this same SO<sub>2</sub> extensive internal and grain boundary oxidation occur in the case of both normal purity Ni-40 wt. % Cr and Ni-40 wt. % Cr-0.5 wt. % Y. Only very limited amounts of internal oxidation effect the high purity Ni-40 wt. % Cr alloy.
- \* For the yttrium-containing Ni-40 wt. % Cr alloy, sulfur is associated with yttrium enrichments in the alloy. However there are many more sulfur-rich precipitates (chromium sulfide particles) that are not associated with any yttrium enrichment.
- \* 1180°C cyclic oxidation experiments were conducted in air to determine if chromium additions to either Ni-25 wt. % Al or Ni-30 wt. % Al alloys would improve oxide scale adherence by producing a "reactive" element effect. Small yttrium additions to the alloys produced adherent scales. However chromium additions in the range of one to seven weight percent had no beneficial effect on oxide scale adherence. In fact, generally such additions debited oxide scale adherence in comparison to behavior observed for the base line alloys.

## VI. REFERENCES

1. D. P. Whittle and J. Stringer, *Philos. Trans. R. Soc. A.*, vol. A295, pp. 309-29 (1980).
2. J. K. Tien and F. S. Pettit, *Metall. Trans.*, vol. 3, pp. 1587-99 (1972).
3. J. E. Antill and K. A. Peakill, *J. Iron and Steel Inst.*, vol. 205, pp. 1587-99 (1972).
4. F. A. Golightly, F. H. Stott and G. C. Wood, *Oxid. of Met.*, vol. 10, pp. 163-87 (1976).
5. H. Pfeiffer, *Werkst. Korros.*, vol. 8, pp. 574-79 (1957).
6. J. E. McDonald and J. B. Eberhart, *Metall. Trans.*, vol. 233, pp. 512-17 (1965).
7. A. W. Funkenbusch, J. G. Smeggil and N. S. Bornstein, *Metall. Trans.*, vol. 16A, pp. 1164-66 (1985).
8. J. G. Smeggil, A. W. Funkenbusch and N. S. Bornstein, *Metall. Trans.*, vol. 17A, pp. 923-32 (1986).
9. J. G. Smeggil, "Study of Adherent Oxide Scales," Report No. 89-917259-1, Contract No. N00014-85-C-0421, United Technologies Research Center, E. Hartford, Connecticut 01608, February 15, 1989.
10. C. L. Briant and K. L. Luthra, *Metall. Trans.*, vol. 19A, pp. 2099-2108 (1988).
11. J. L. Smialek and R. Browning, *Proceedings of high Temperature materials Chemistry III*, vol. 86-2, pp. 258-72 (1986), published by the Electrochemical Society, Fall Meeting of the Electrochemistry Society, Los Vegas, Nevada (1985).
12. C. G. H. Walker and M. M. El Gomati, *Applied Surface Science*, vol. 35, pp. 164-72 (1988-89).
13. J. G. Smeggil and G. G. Peterson, *Oxid. of Metals*, vol. 29, pp. 103-119 (1988).
14. J. G. Smeggil, *Materials Science and Engineering*, vol. 87, pp. 261-266 (1987).
15. J. L. Smialek, *Metall. Trans.*, vol. 18A, pp. 164-77 (1987).



A. CRUCIBLE USED TO CONTAIN NORMAL PURITY SPECIMEN



B. CRUCIBLE USED TO CONTAIN HIGH PURITY (LOW SULFUR) SPECIMEN

**Fig. 1** Alumina crucibles used to separately hold N-40 wt % Cr specimens at 1000°C for 100 hours in stagnant air. Discoloration at base of crucible results from chromium oxide volatilization from normal purity Ni-40 wt % Cr, cf. arrows in A.

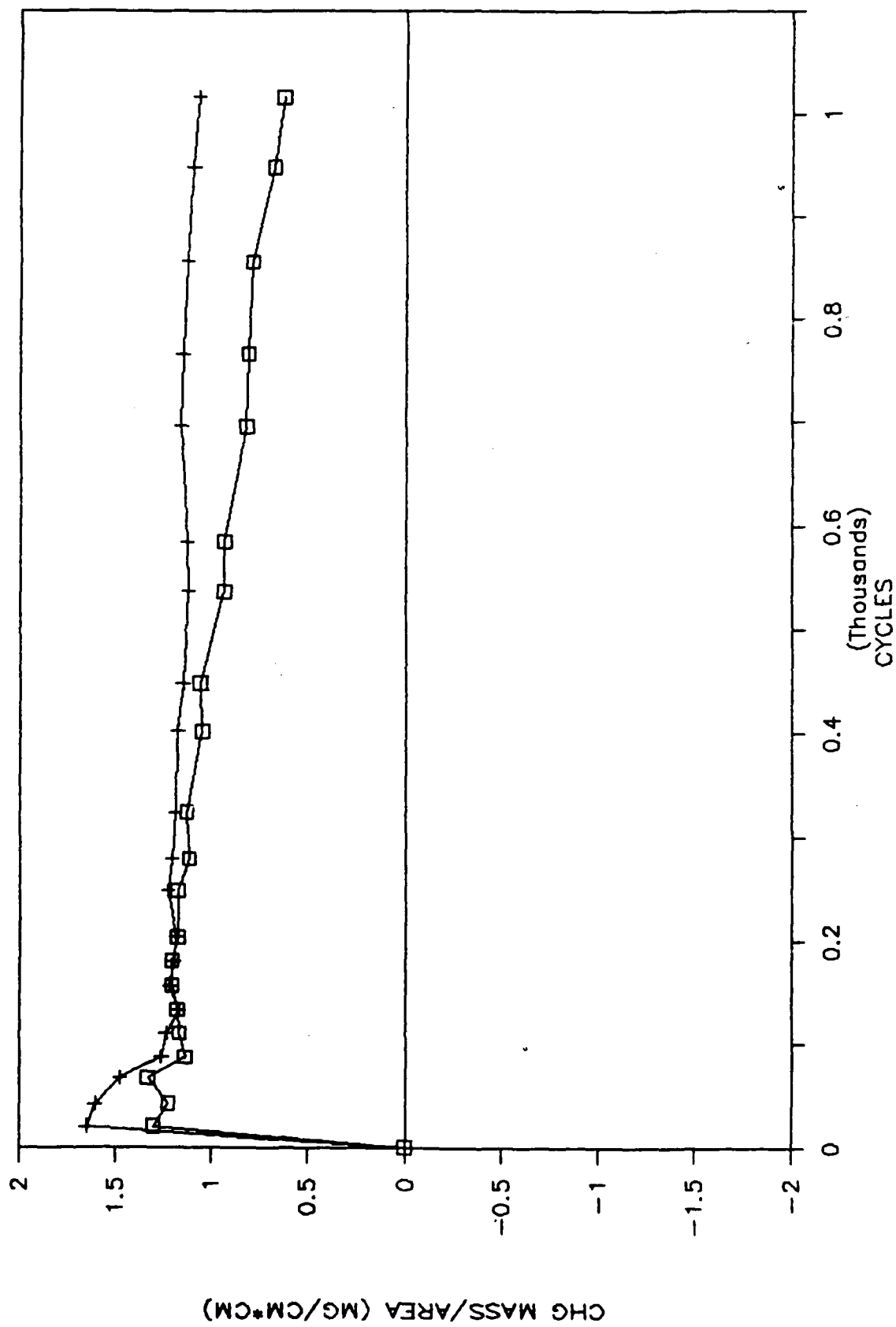


Figure 2 Normal purity Ni-40 wt. % Cr cyclically oxidized to 1000°C in 0.1% SO<sub>2</sub>-O<sub>2</sub> for 1016 cycles.

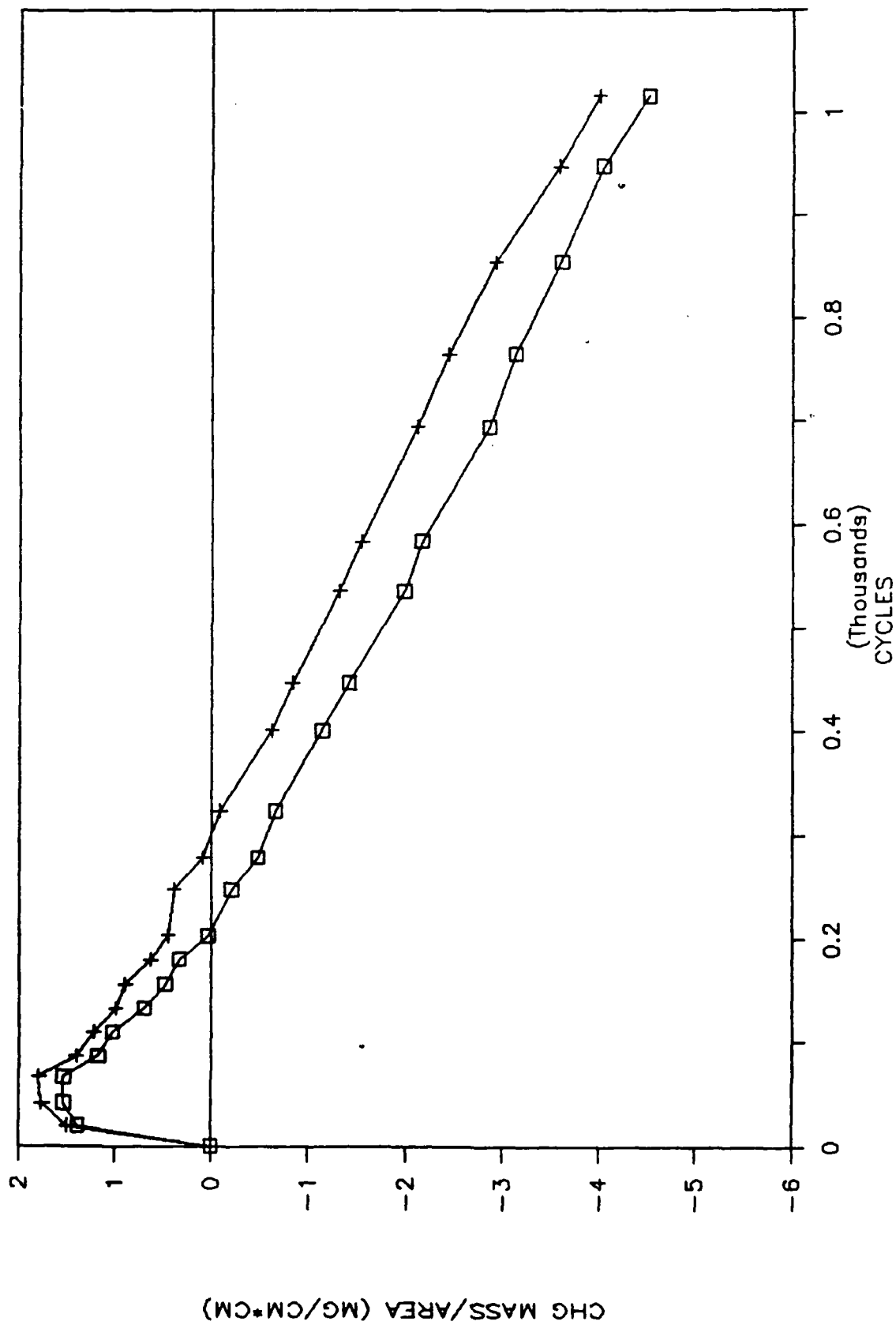


Figure 3 High purity (low sulfur) Ni-40 wt. % Cr cyclically oxidized to 1000°C in 0.1% SO<sub>2</sub>-O<sub>2</sub> for 1016 cycles.

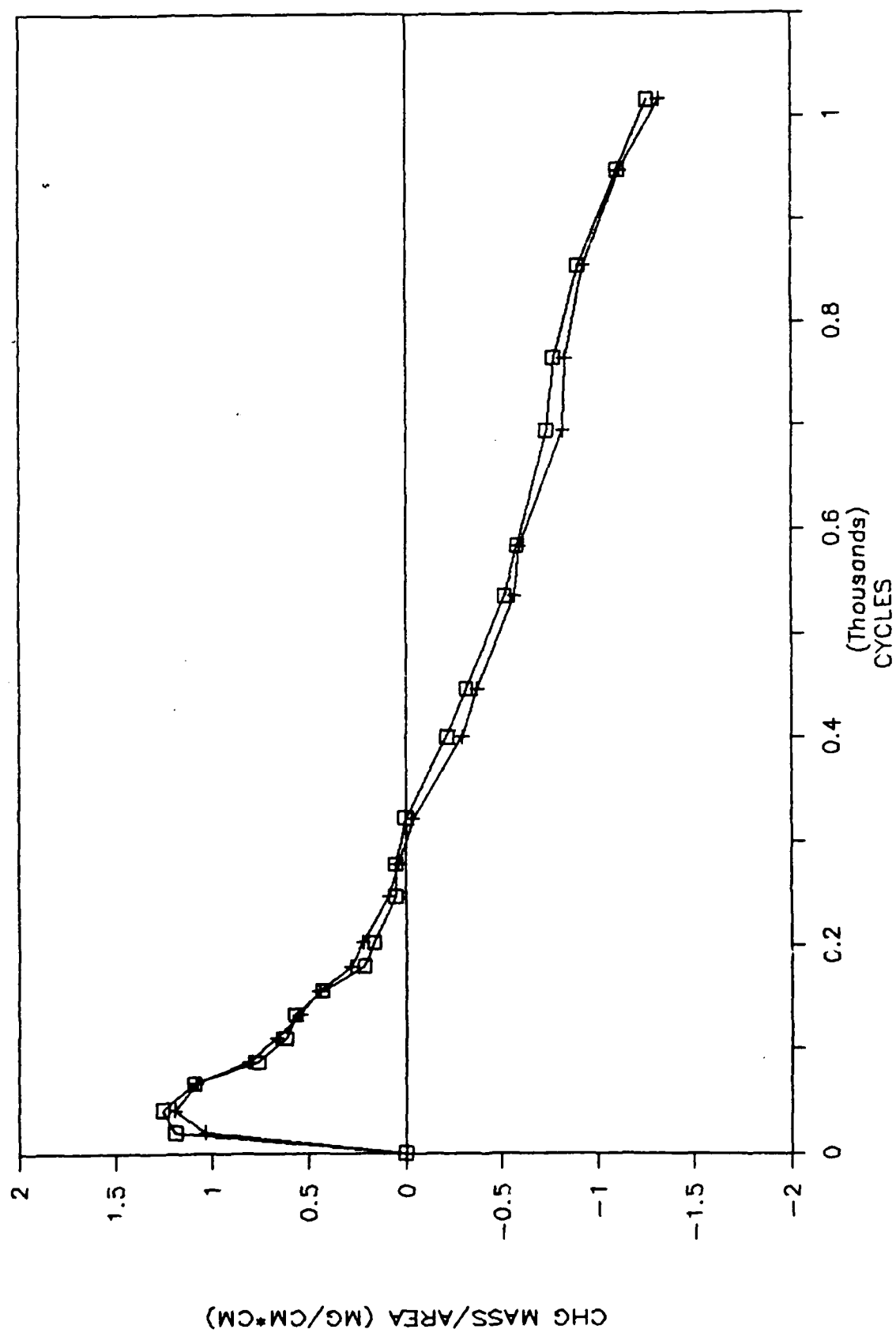


Figure 4 Ni-40 wt. % Cr-0.5 wt. % Y cyclically oxidized to 1000°C in 0.1% SO<sub>2</sub>-O<sub>2</sub> for 1016 cycles.

R89-917259-2

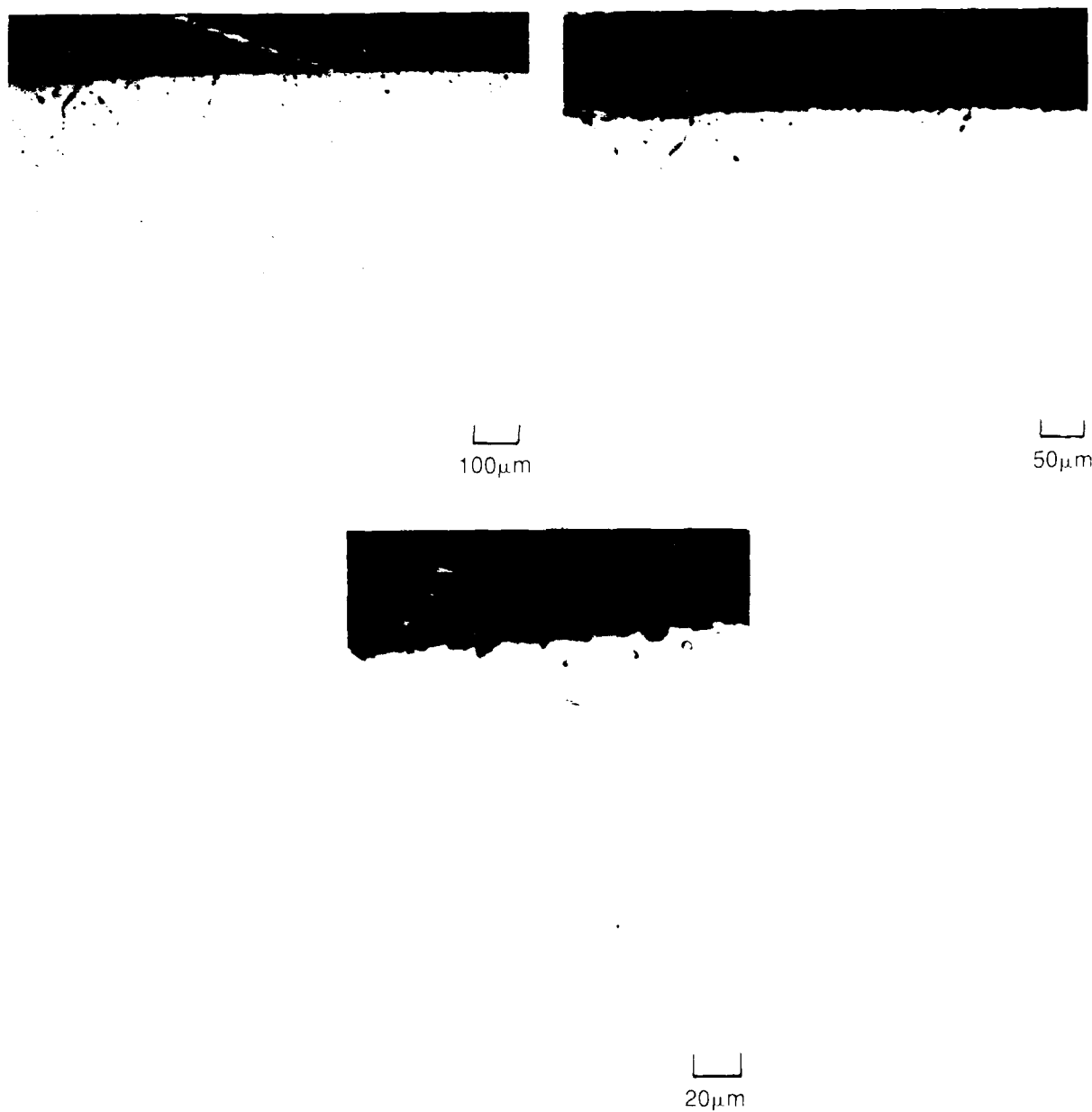
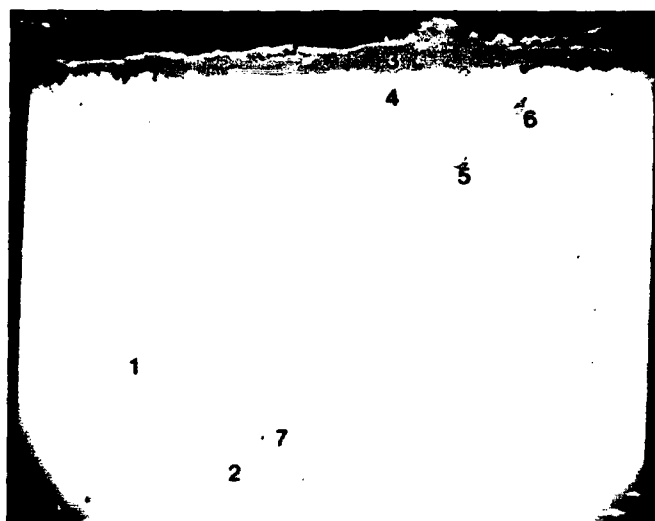


Fig. 5 Normal purity Ni-40 wt % Cr cyclically oxidized to 1000°C in 0.1% SO<sub>2</sub>-O<sub>2</sub> for 1016 cycles. Optical micrograph.

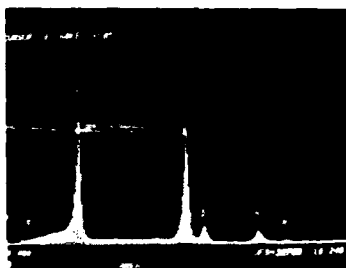
89-10-27-2

R89-917259-2

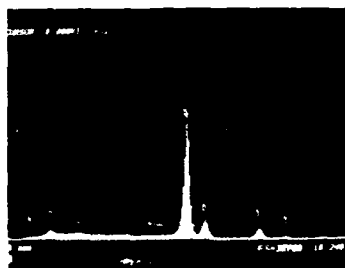


A. BACK SCATTERED ELECTRON MICROGRAPH

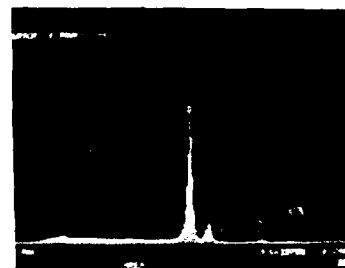
25μm



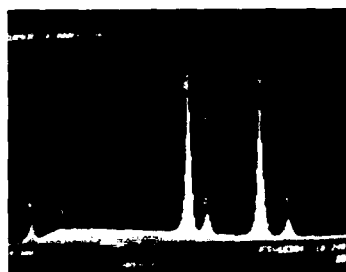
B. EDS (ENERGY DISPERSIVE SPECTRUM) OF AREA 1. cf. A



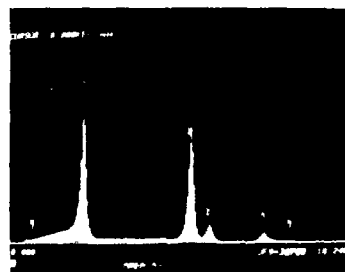
C. EDS OF AREA 2. cf. A



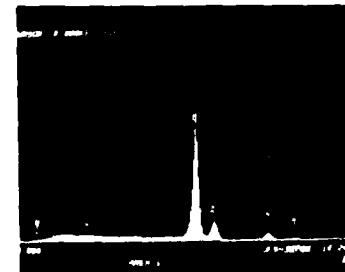
D. EDS OF AREA 3. cf. A.



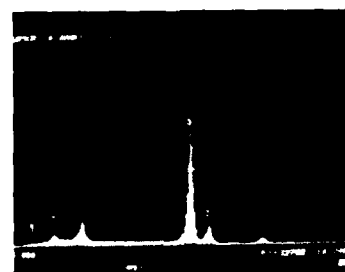
E. EDS OF AREA 4. cf. A



F. EDS OF AREA 5. cf. A



G. EDS OF AREA 6. cf. A



H. EDS OF AREA 7. cf. A

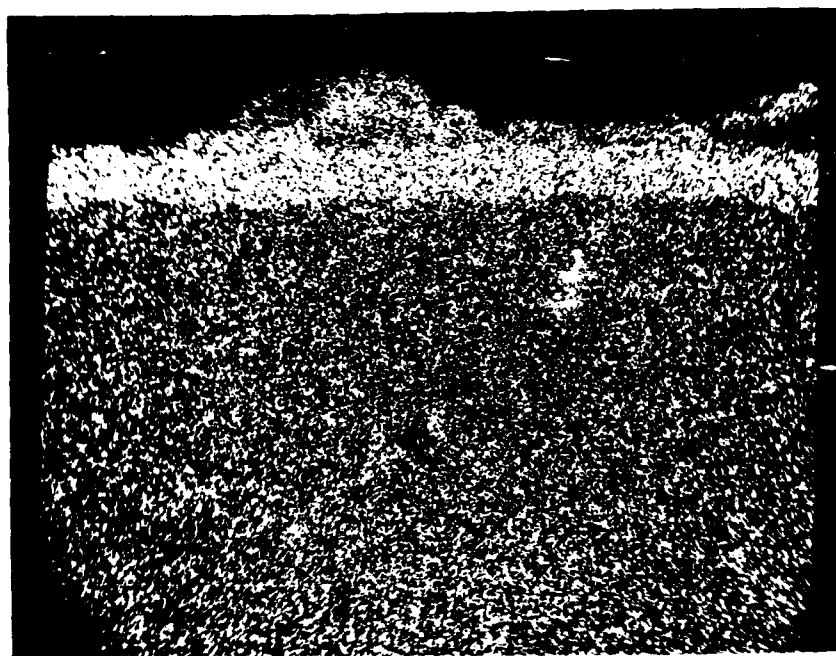
Fig. 6 Normal purity Ni-40 wt % Cr cyclically oxidized to 1000°C in 0.1% SO<sub>2</sub>-O<sub>2</sub> for 1016 cycles.

89-10-27-3

R89-917259-2



A. BACK SCATTERED ELECTRON MICROGRAPH 12.5μm

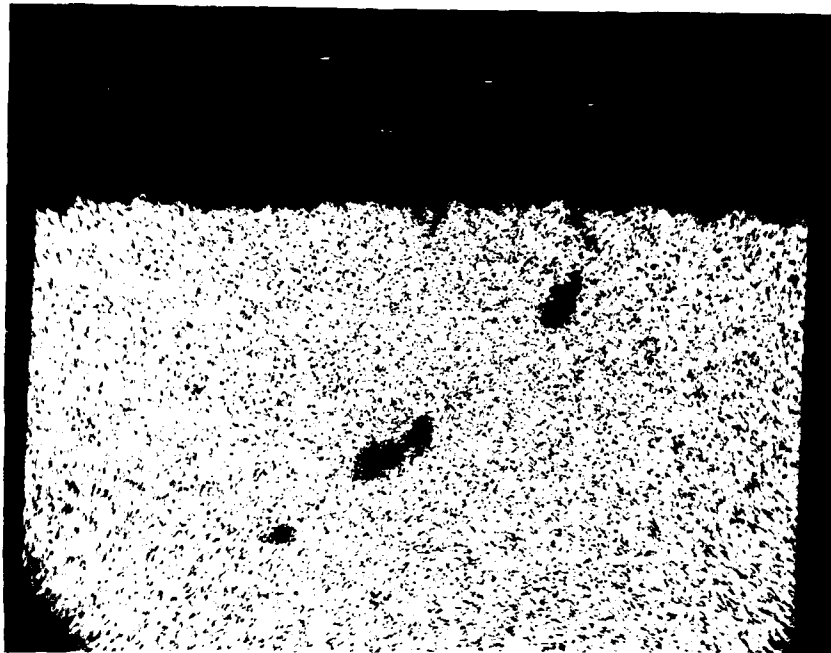


B. X-RAY MAP, CHROMIUM 12.5μm

Fig. 7 Normal purity Ni-40 wt % Cr cyclically oxidized to 1060°C for 1016 cycles in 0.1%  $\text{SO}_2\text{-O}_2$

89-10-27-13

R89-917259-2



C. X-RAY MAP: NICKEL

12.5 μm



D. X-RAY MAP: OXYGEN

12.5 μm

Fig. 7 (cont.) Normal purity Ni-40 wt % Cr cyclically oxidized to 1000°C for 1016 cycles in 0.1% SO<sub>2</sub>-O<sub>2</sub>

89-10-27-14

R89-917259-2

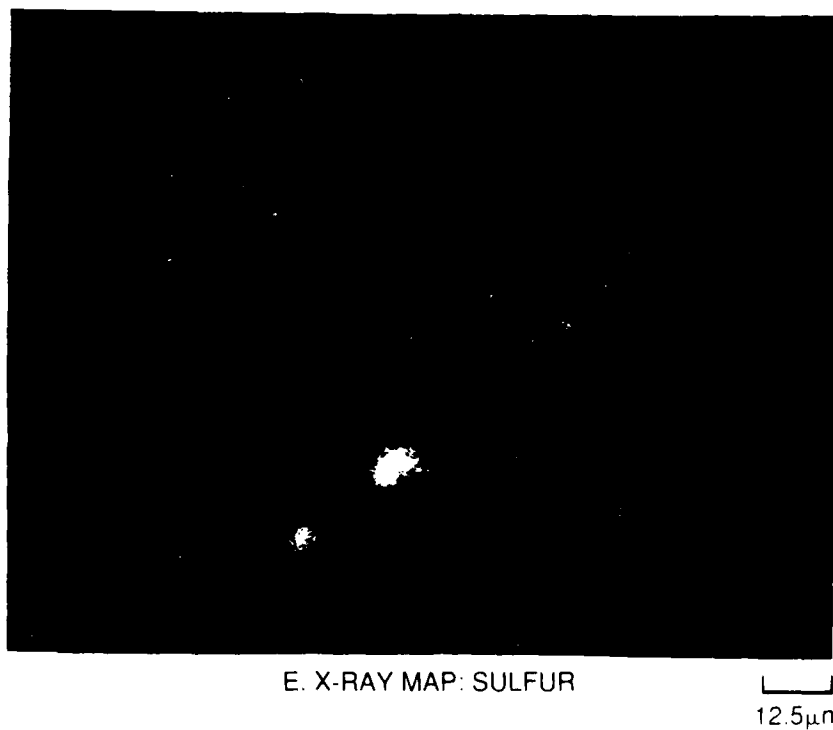


**Fig. 7 (concl'd) Normal purity Ni-40 wt % Cr cyclically oxidized to 1000°C for 1016 cycles in 0.1% SO<sub>2</sub>-O<sub>2</sub>**

89-10-27-15

R89-917259-2

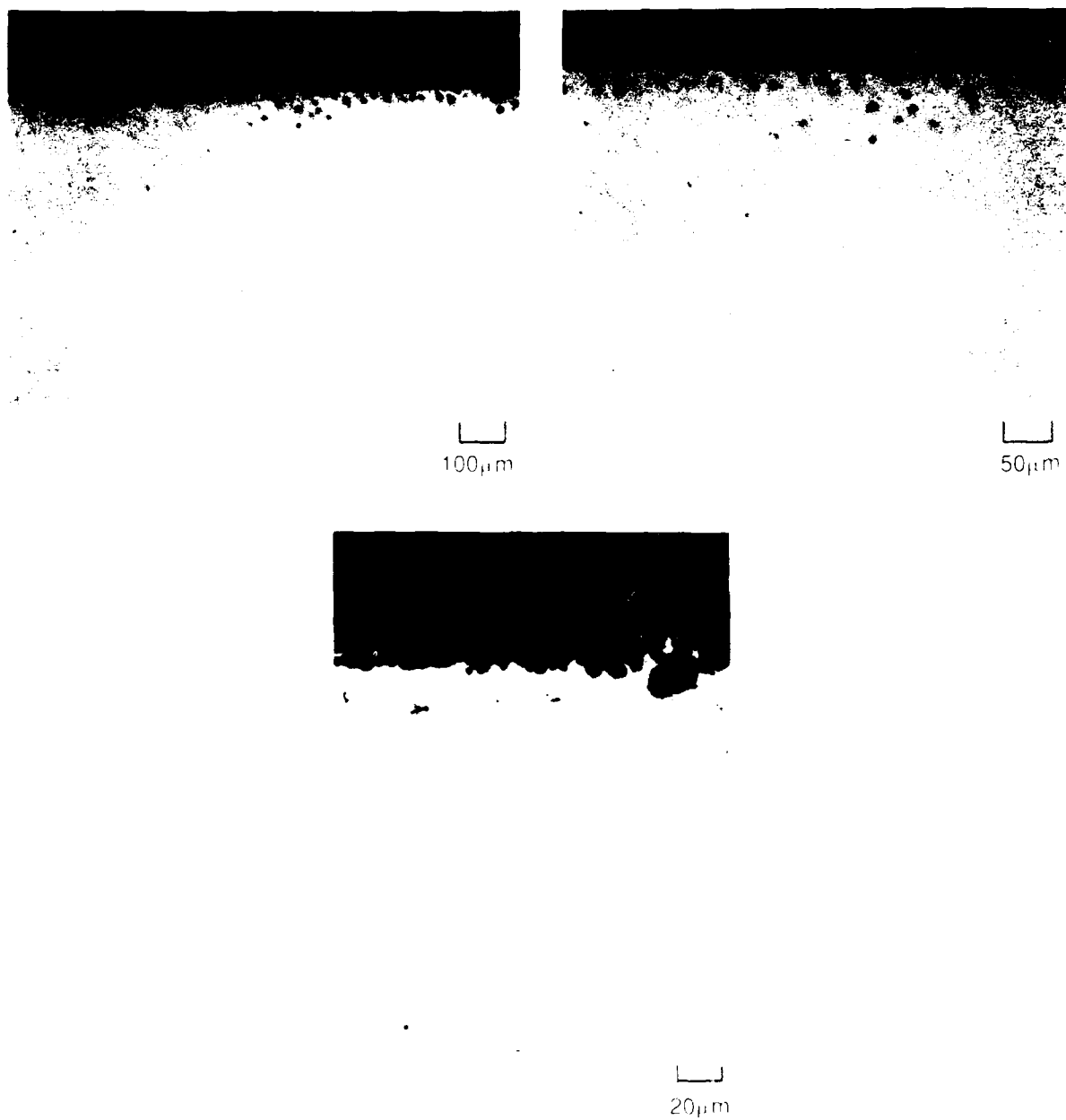


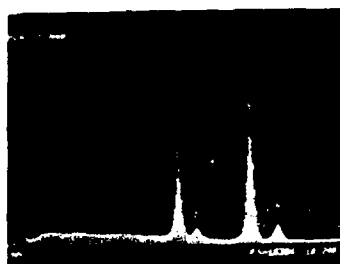
Fig. 8 High purity (low sulfur) Ni-40 wt % Cr cyclically oxidized to 1000°C in 0.1%  $\text{SO}_2$ - $\text{O}_2$  for 1016 cycles. Optical micrographs.

R89-917259-2

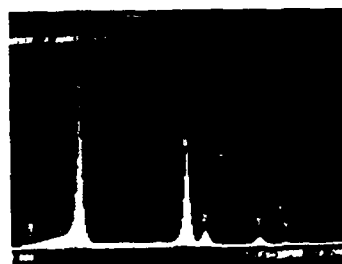


A. BACKSCATTERED ELECTRON MICROGRAPH

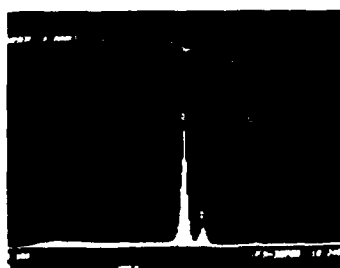
12.5 $\mu$ m



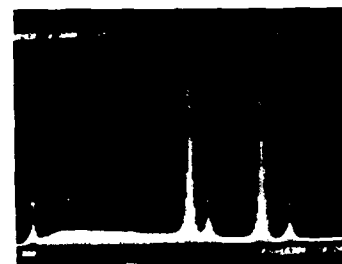
B. EDS (ENERGY DISPERSIVE SPECTRUM)  
OF AREA 1, cf. A



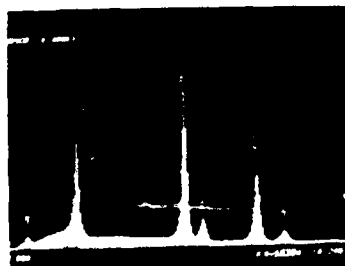
C. EDS OF AREA 2, cf. A



D. EDS OF AREA 3, cf. A



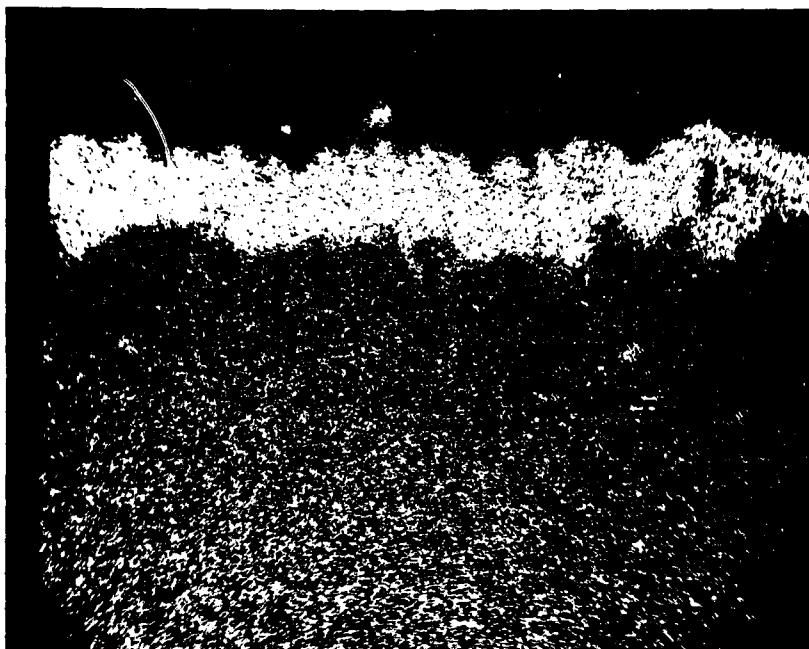
E. EDS OF AREA 4, cf. A



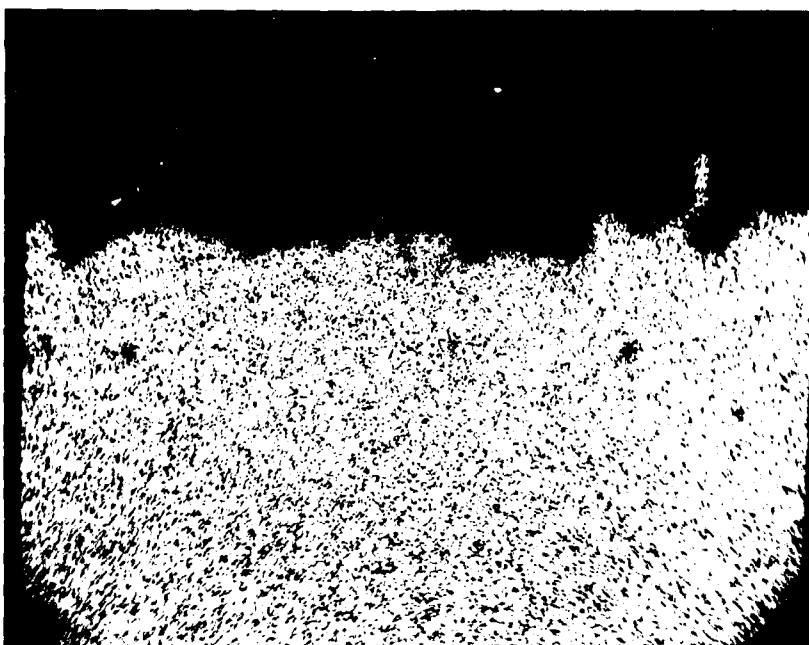
F. EDS OF AREA 5, cf. A

Fig. 9 High purity (low sulfur) Ni-40 wt % Cr cyclically oxidized to 1000°C in 0.1%  $\text{SO}_2\text{-O}_2$  for 1016 cycles.

89-10-27-7



G. X-RAY MAP: CHROMIUM, cf. A

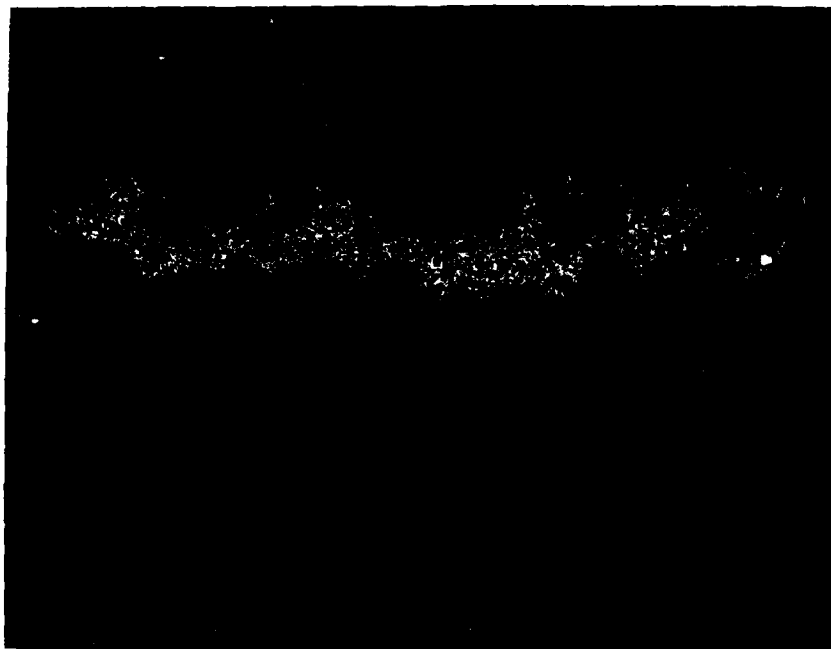


H. X-RAY MAP: NICKEL, cf. A

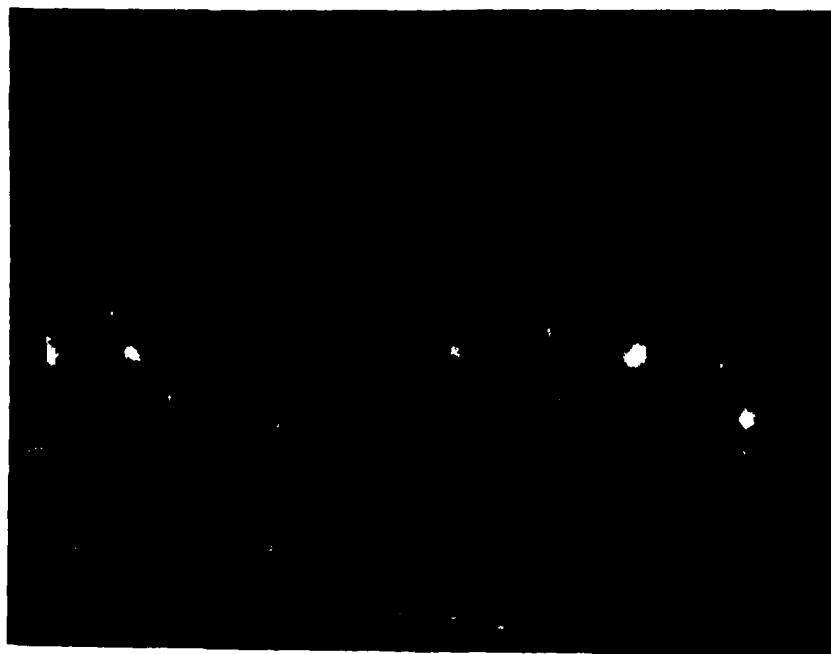
15 $\mu$ m

Fig. 9 (cont.) High purity (low sulfur) Ni-40 wt % Cr cyclically oxidized to 1000°C in 0.1 % SO<sub>2</sub>-O<sub>2</sub> for 1016 cycles.

R89-917259-2



I. X-RAY MAP: OXYGEN, cf. A



J. X-RAY MAP: SULFUR, cf. A

15 $\mu$ m

Fig. 9 (concl'd) High purity (low sulfur) Ni-40 wt % Cr cyclically oxidized to 1000°C in 0.1 % SO<sub>2</sub>-O<sub>2</sub> for 1016 cycles.

89-10-27-9

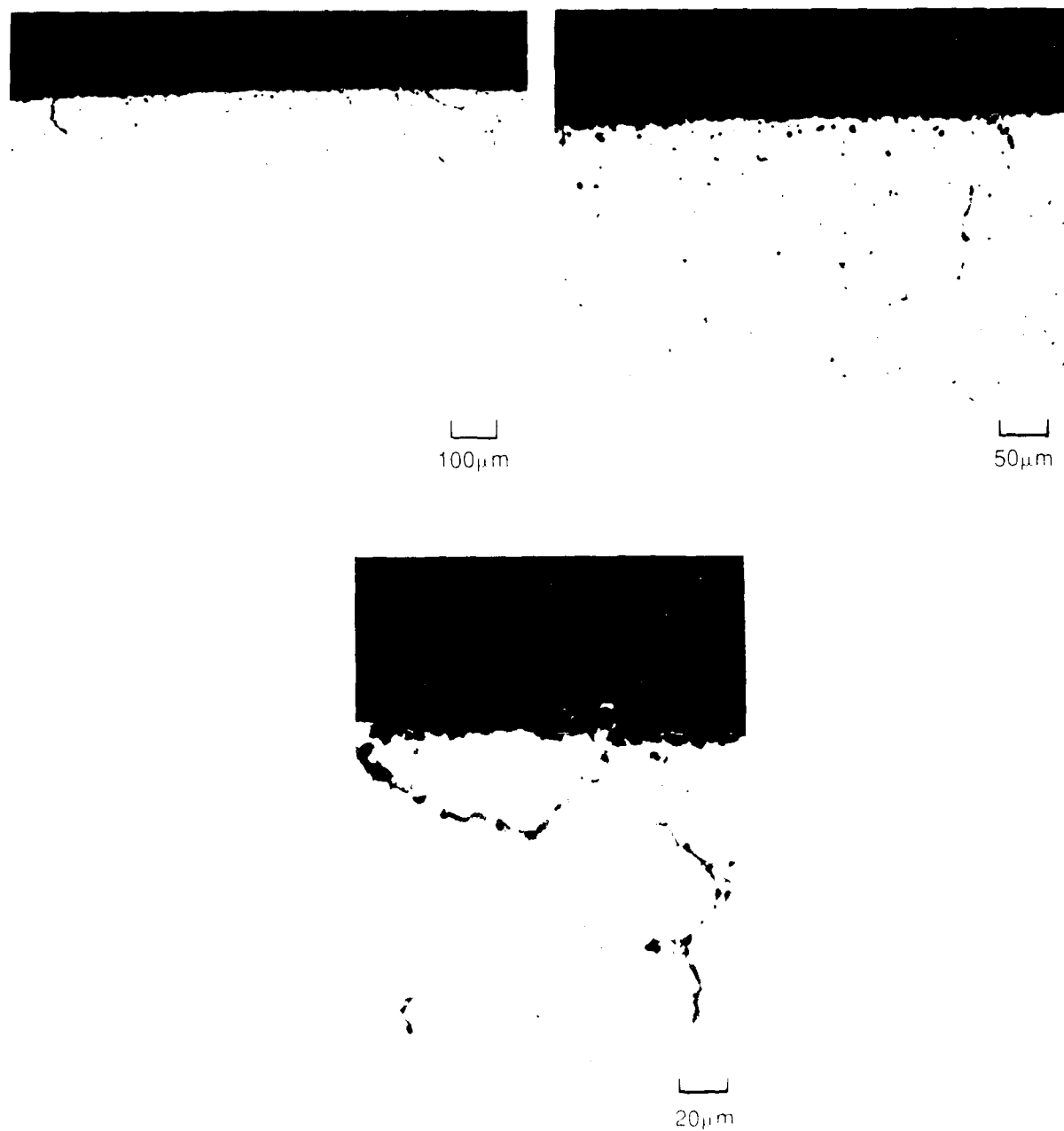


Fig. 10 Ni-40 wt % Cr-0.5 wt % Y cyclically oxidized to 1000°C in 0.1% SO<sub>2</sub>-O<sub>2</sub> for 1016 cycles. Optical micrographs.

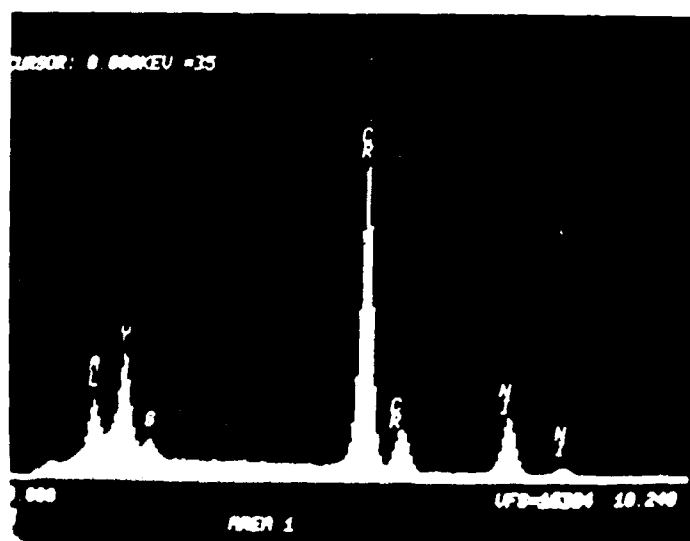
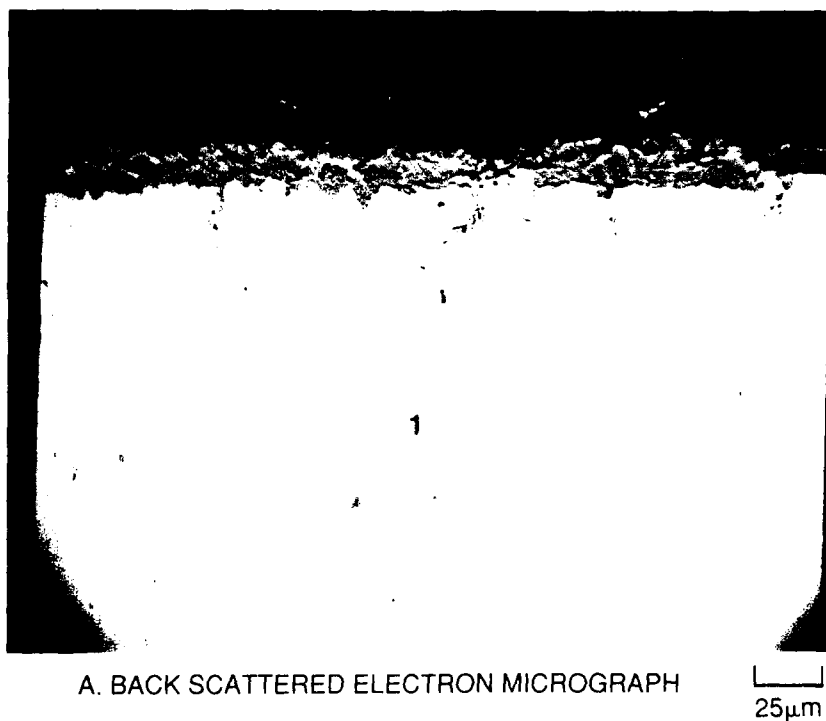
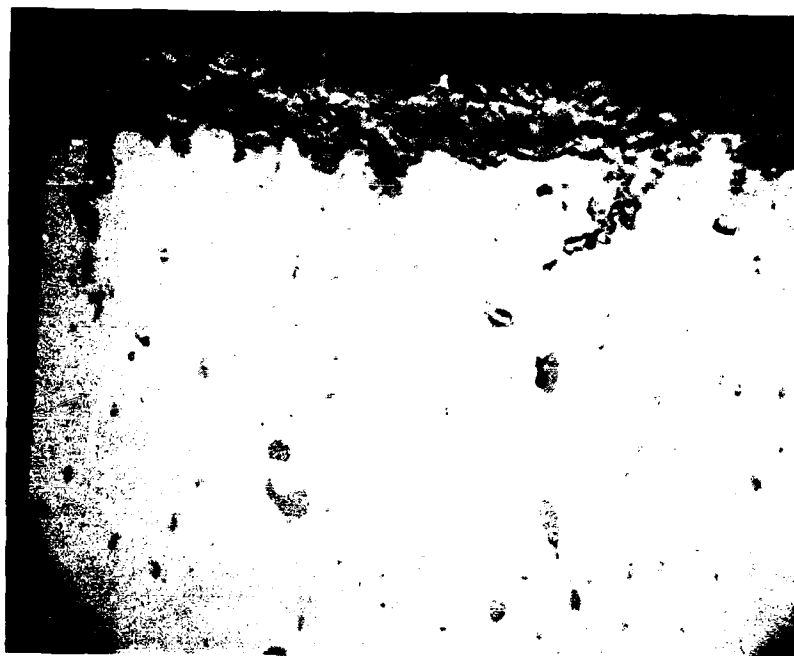
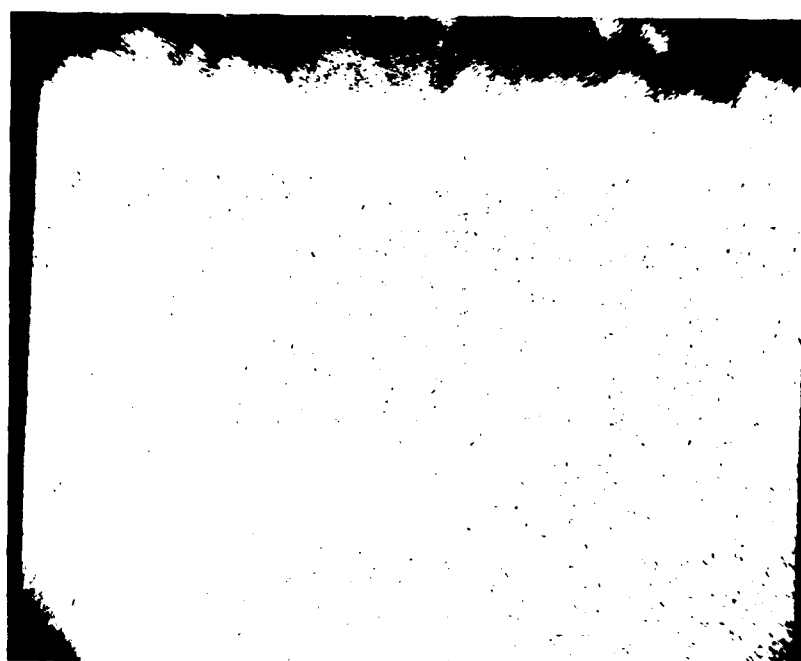


Fig. 11 Ni-40 wt % Cr-0.5 wt % Y cyclically oxidized to 1000°C in 0.1%  $\text{SO}_2\text{-O}_2$  for 1016 cycles.



A. BACK SCATTERED ELECTRON MICROGRAPH

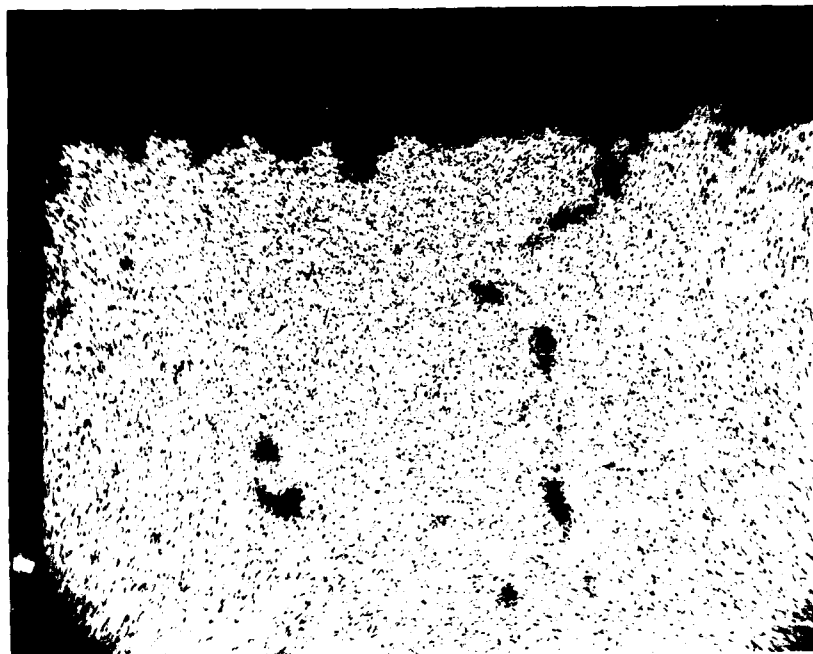
15 μm



B. X-RAY MAP: CHROMIUM

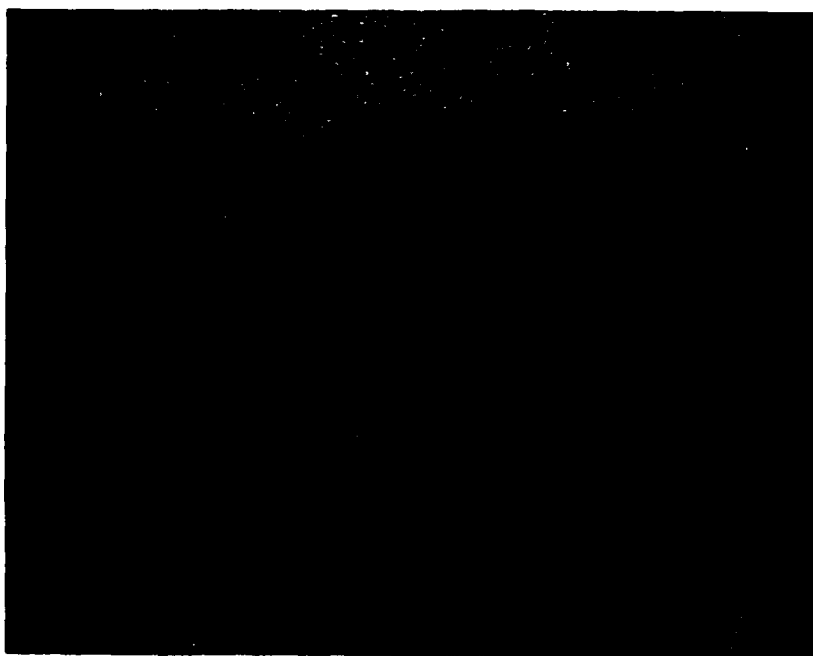
15 μm

Fig. 12 Ni-40 wt % Cr-0.5 wt % Y cyclically oxidized to 1000°C in 0.1% SO<sub>2</sub>-O<sub>2</sub> for 1016 cycles.



C. X-RAY MAP: NICKEL

15μm

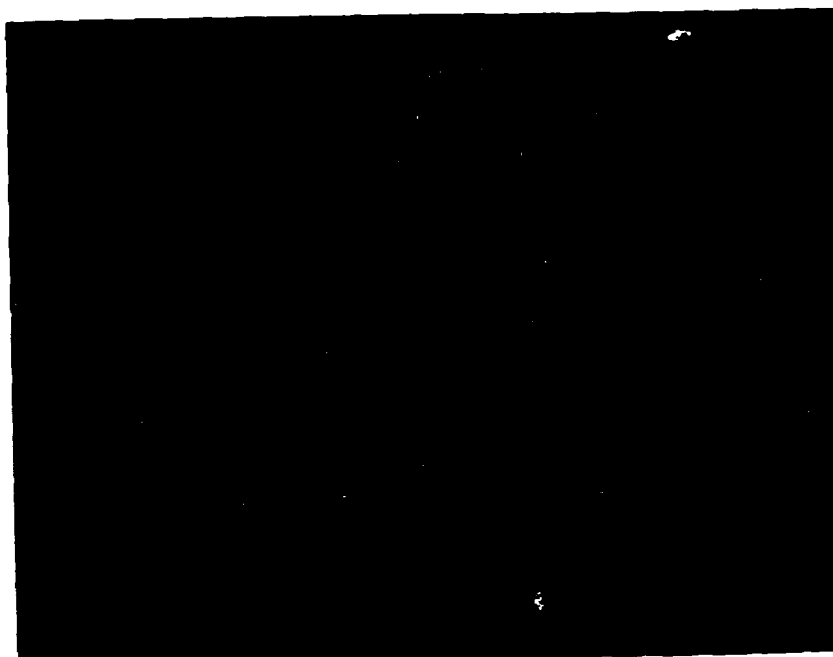


D. X-RAY MAP: OXYGEN

15μm

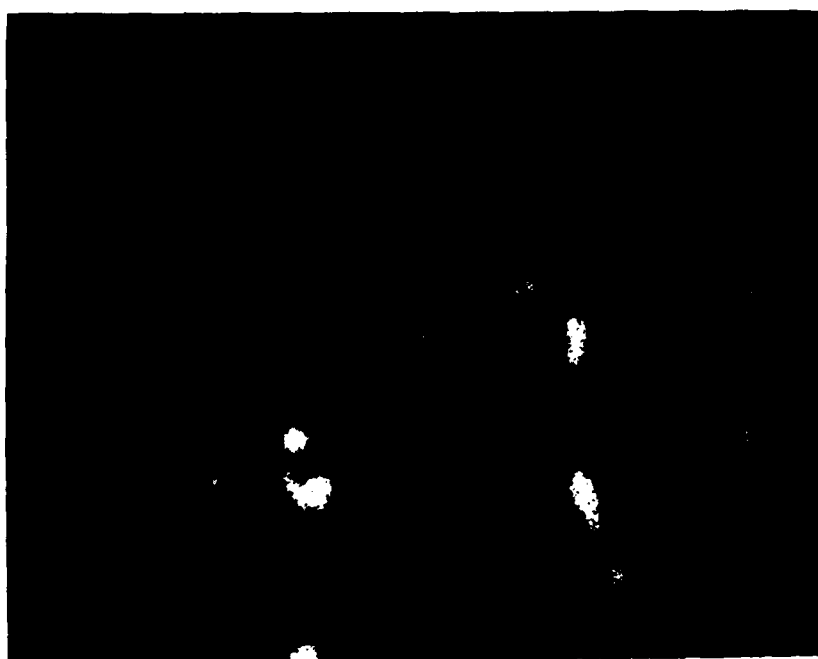
Fig. 12 (cont.) Ni-40 wt % Cr-0.5 wt % Y cyclically oxidized to 1000°C in 0.1% SO<sub>2</sub>-O<sub>2</sub> for 1016 cycles.

R89-917259-2



E. X-RAY MAP: YTTRIUM

15 $\mu$ m



F. X-RAY MAP: SULFUR

15 $\mu$ m

Fig. 12 (concl'd) Ni-40 wt % Cr-0.5 wt % Y cyclically oxidized to 1000°C in 0.1% SO<sub>2</sub>-O<sub>2</sub> for 1016 cycles.

89-10-27-12

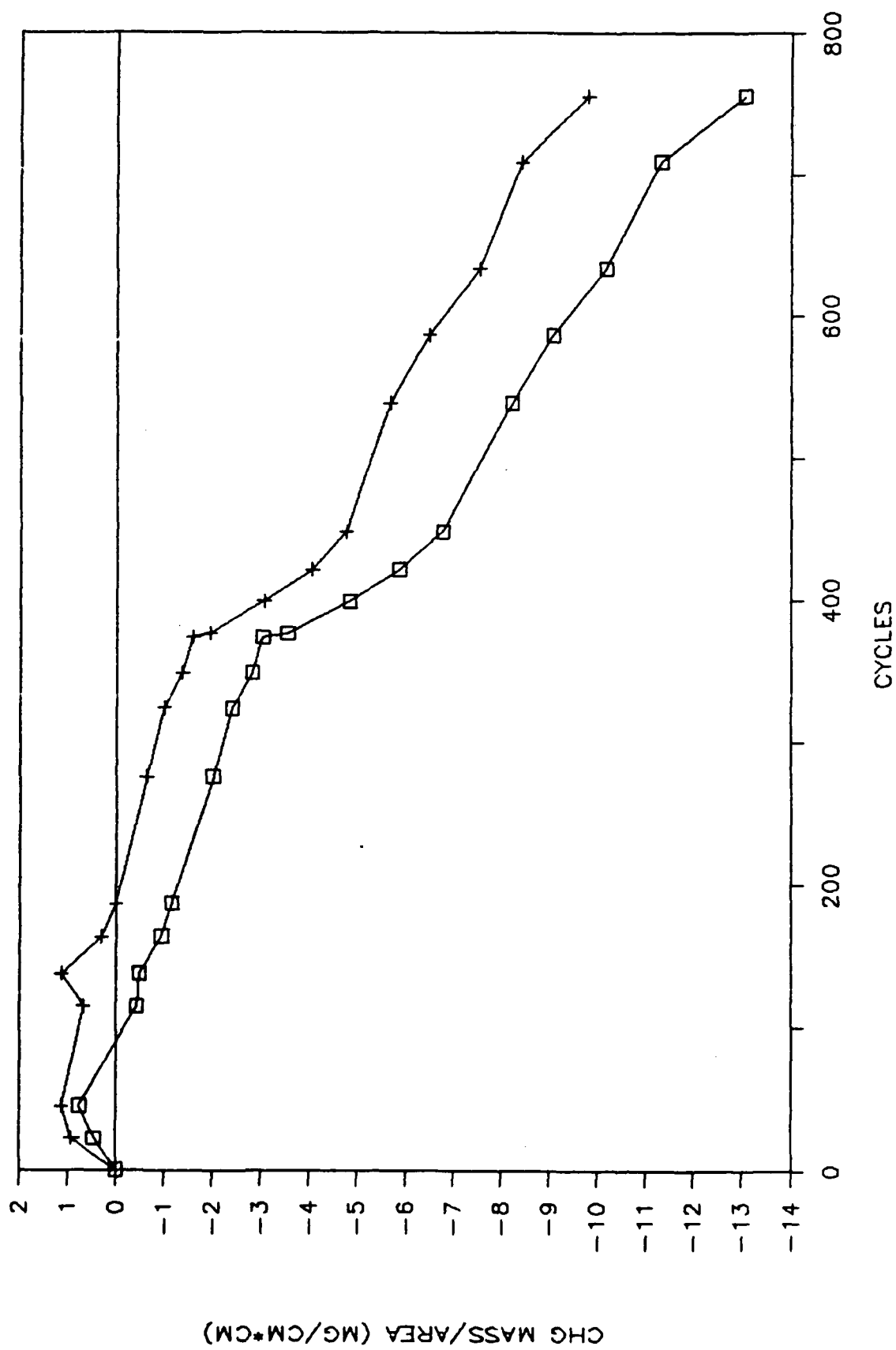


Figure 13 1180°C cyclic oxidation test results for Ni-25 wt. %Al.

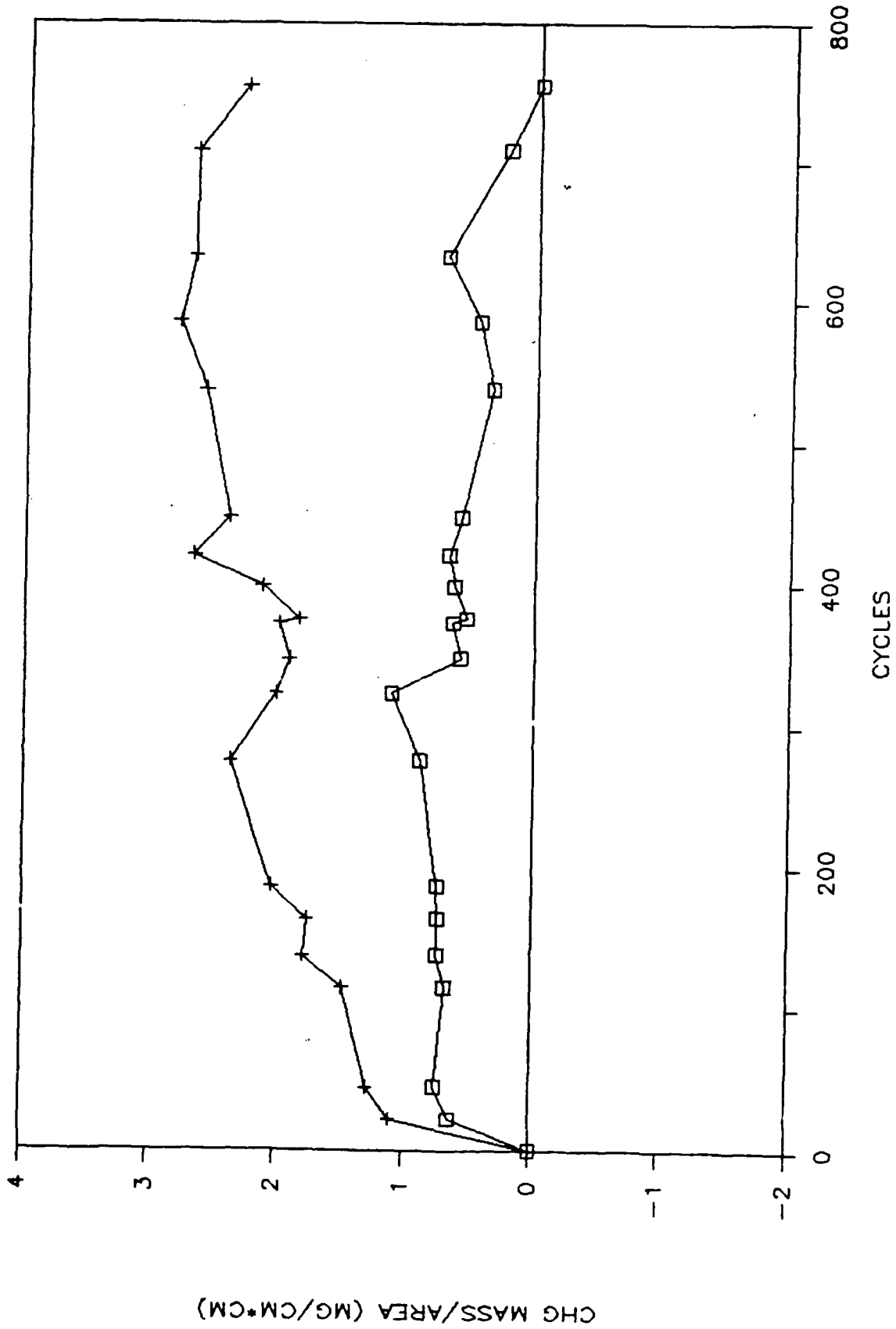


Figure 14 1180°C cyclic oxidation test results for Ni-25 wt. % Al-0.1 wt. % Y.

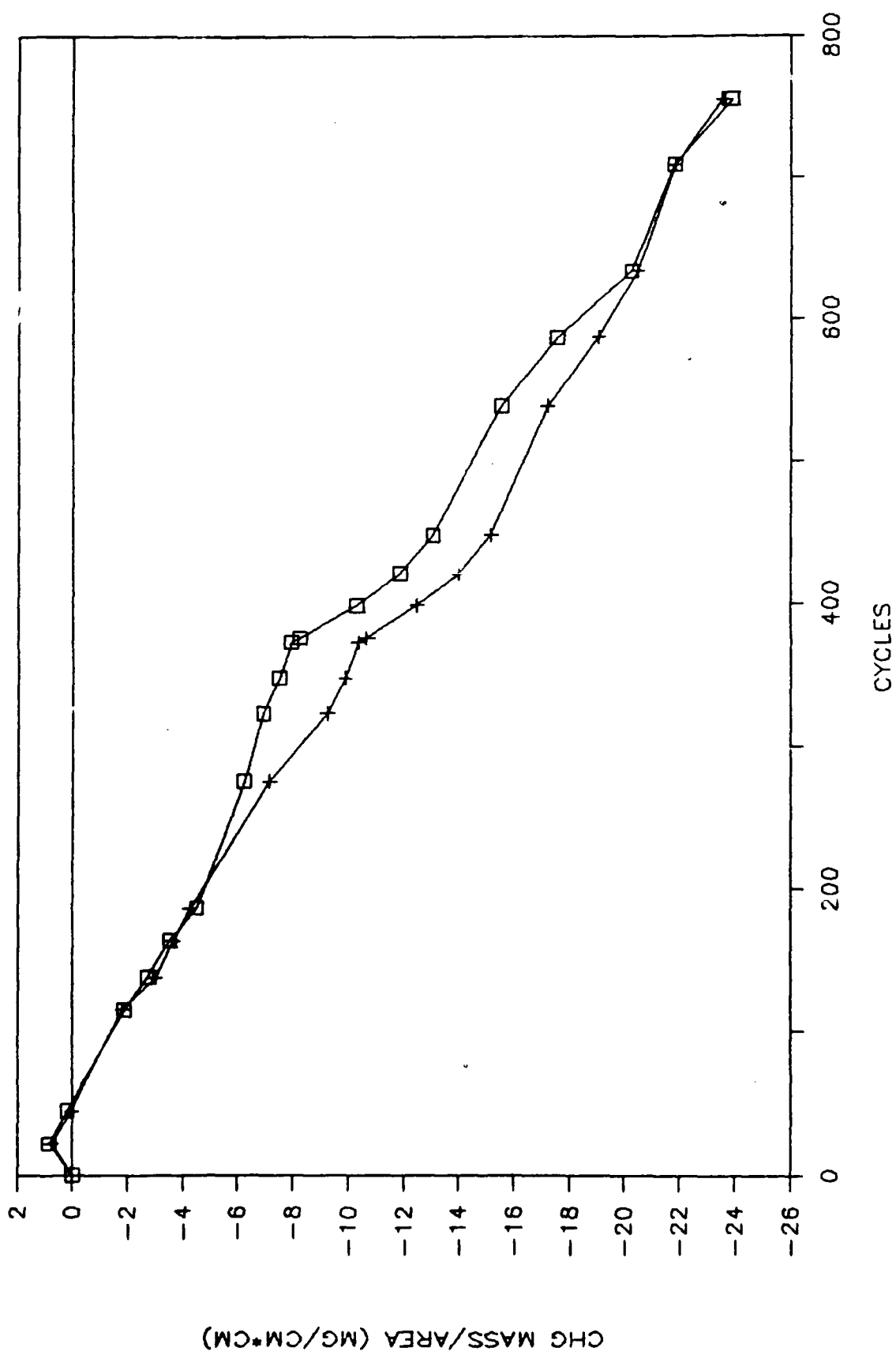


Figure 15 1180°C cyclic oxidation test results for Ni-25 wt. % Al-1 wt. % Cr.

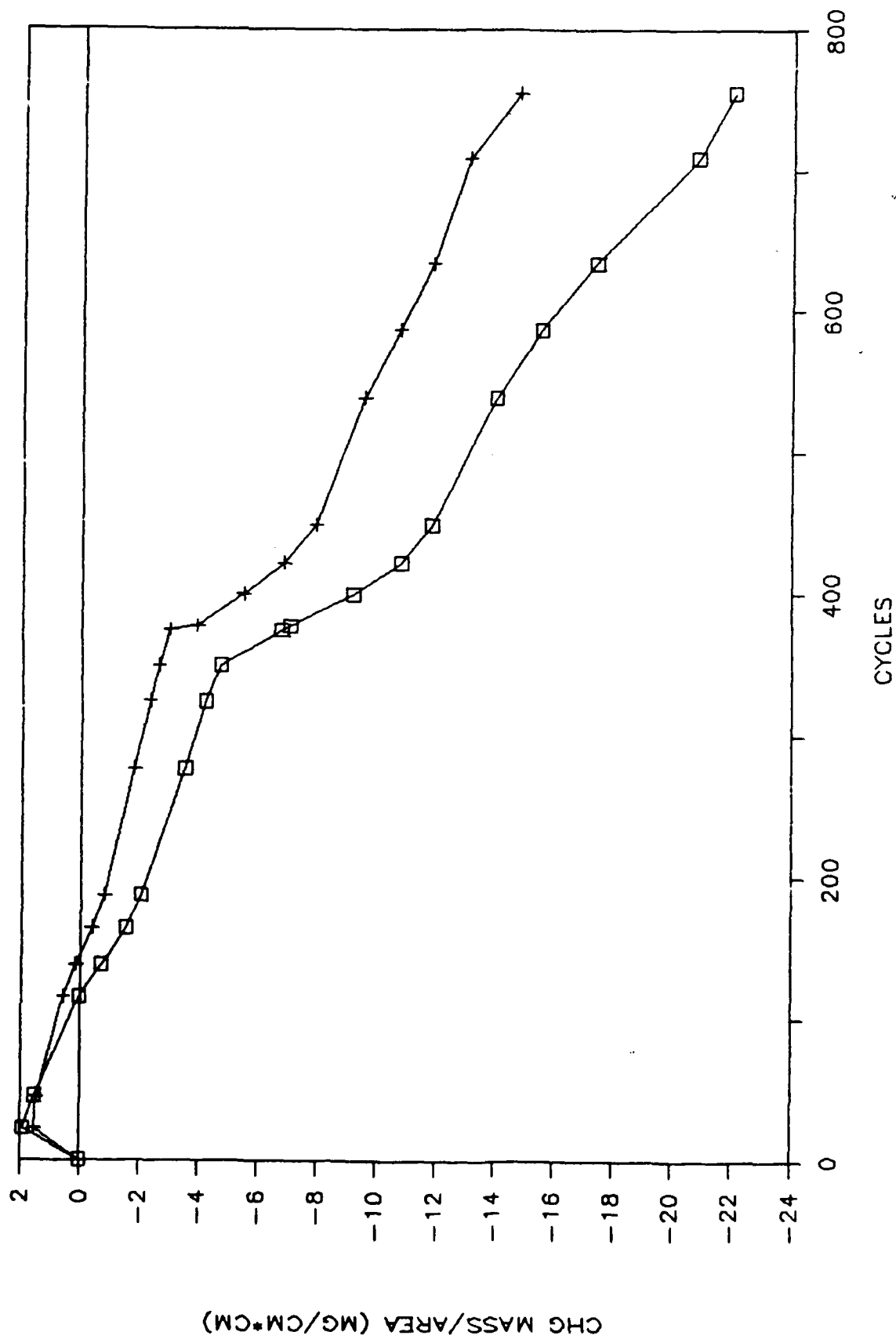


Figure 15 1180°C cyclic oxidation test results for Ni-25 wt. % Al-3 wt. % Cr.

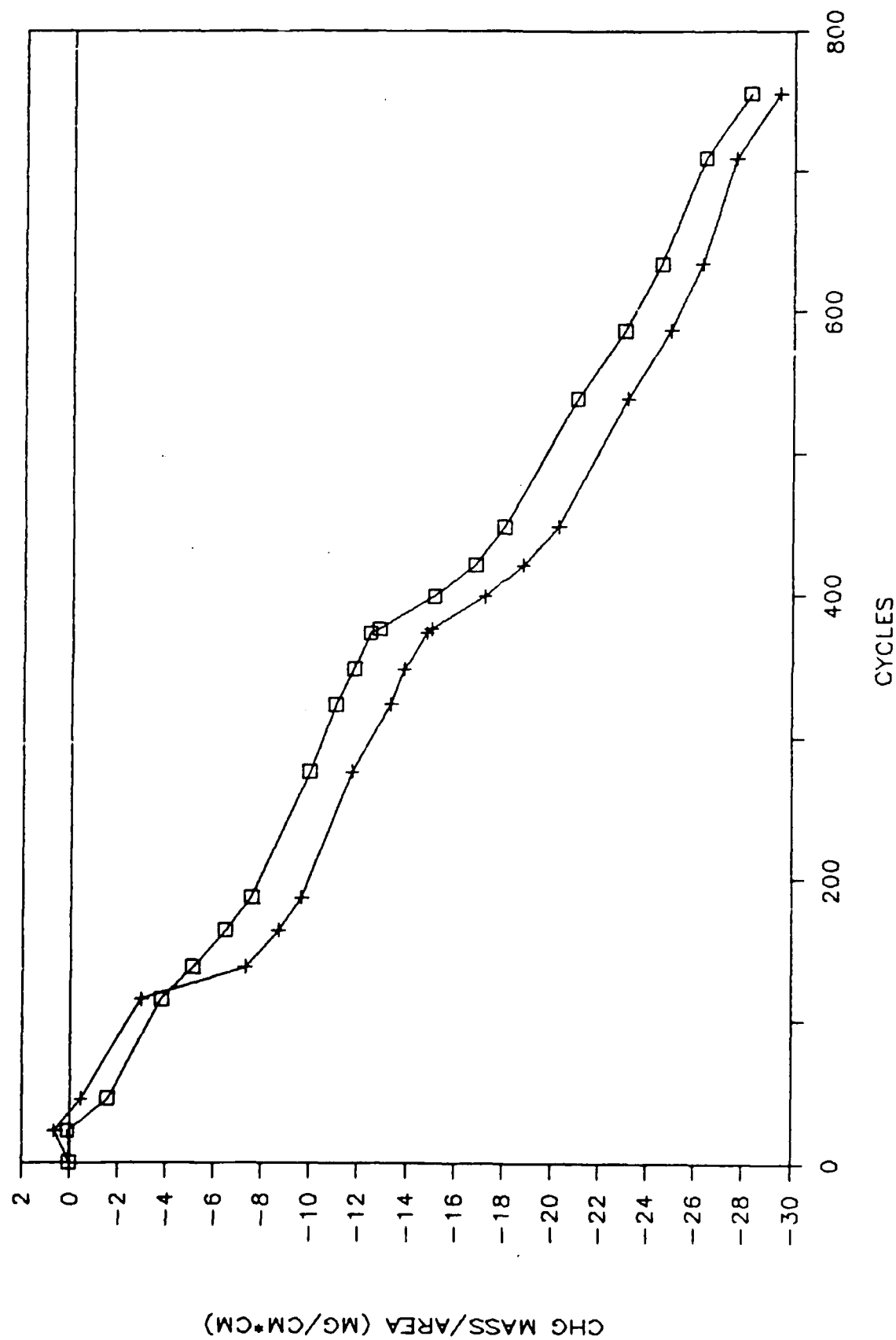


Figure 17 1180°C cyclic oxidation test results for Ni-25 wt. % Al-5 wt. % Cr.

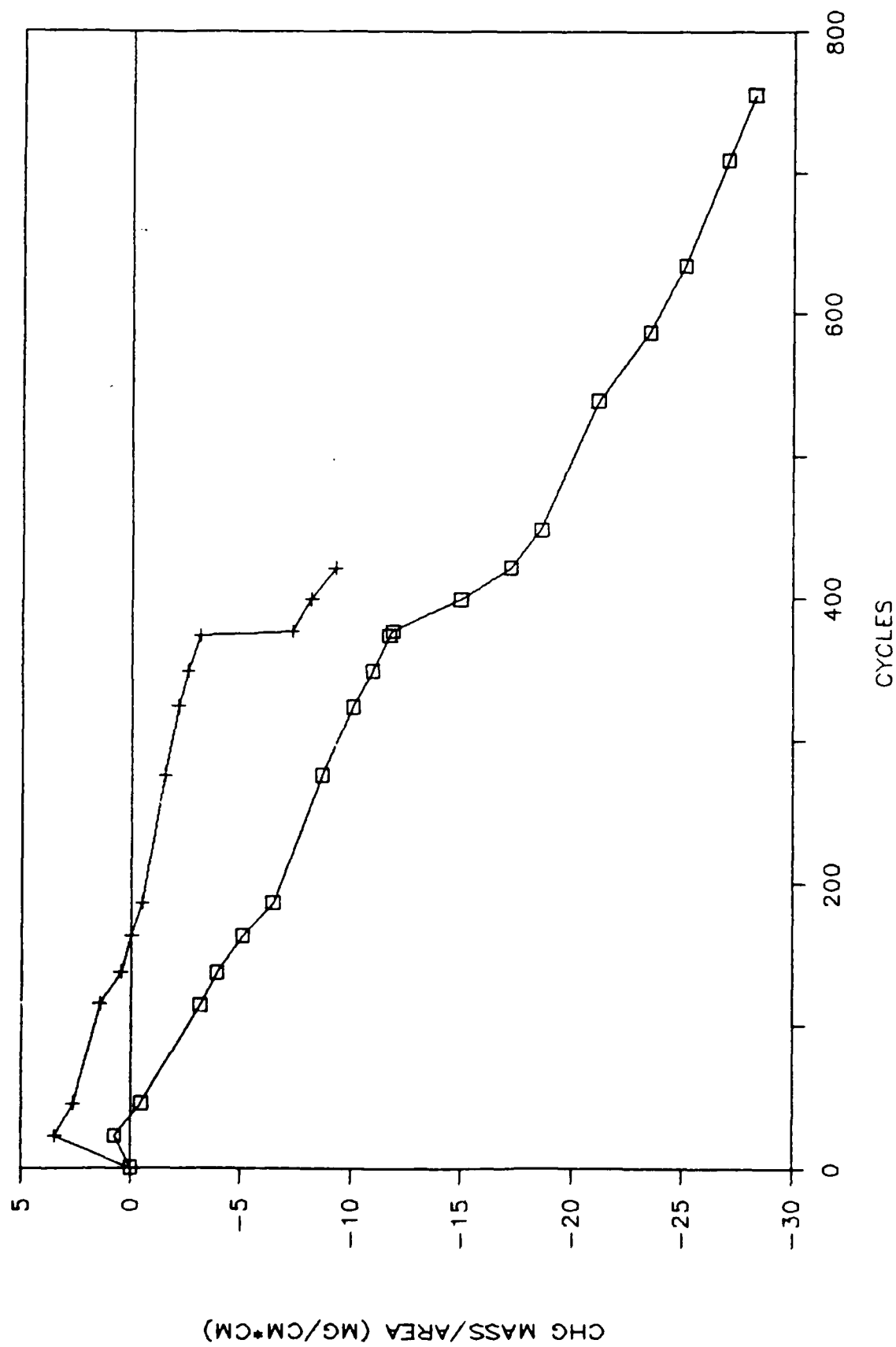


Figure 18 1180°C cyclic oxidation test results for Ni-25 wt. % Al-7 wt. Cr.

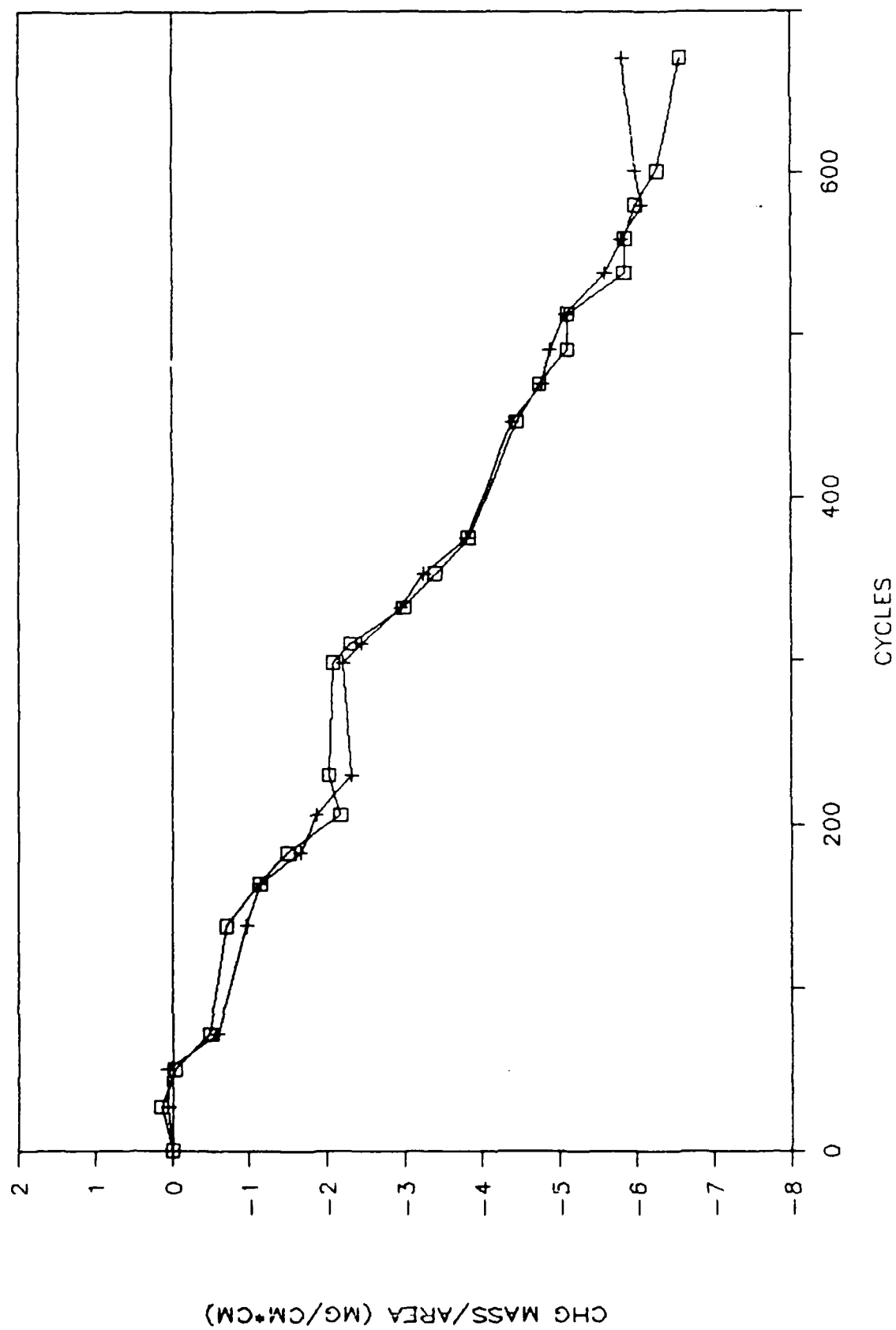


Figure 19 1180°C cyclic oxidation test results for Ni-30 wt. % Al.

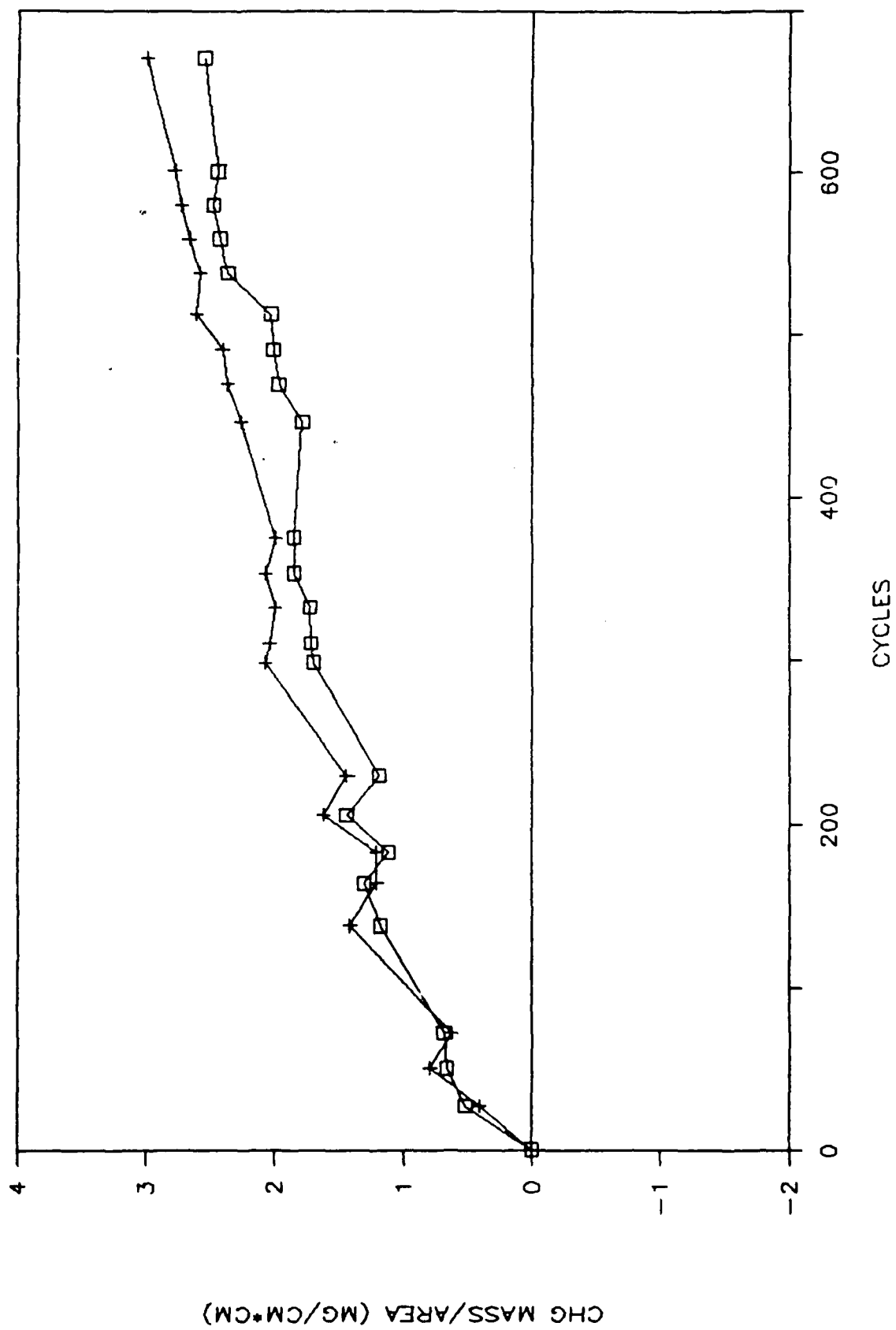


Figure 20 1180°C cyclic oxidation test results for Ni-30 wt. % Al-0.1 wt. % Y.

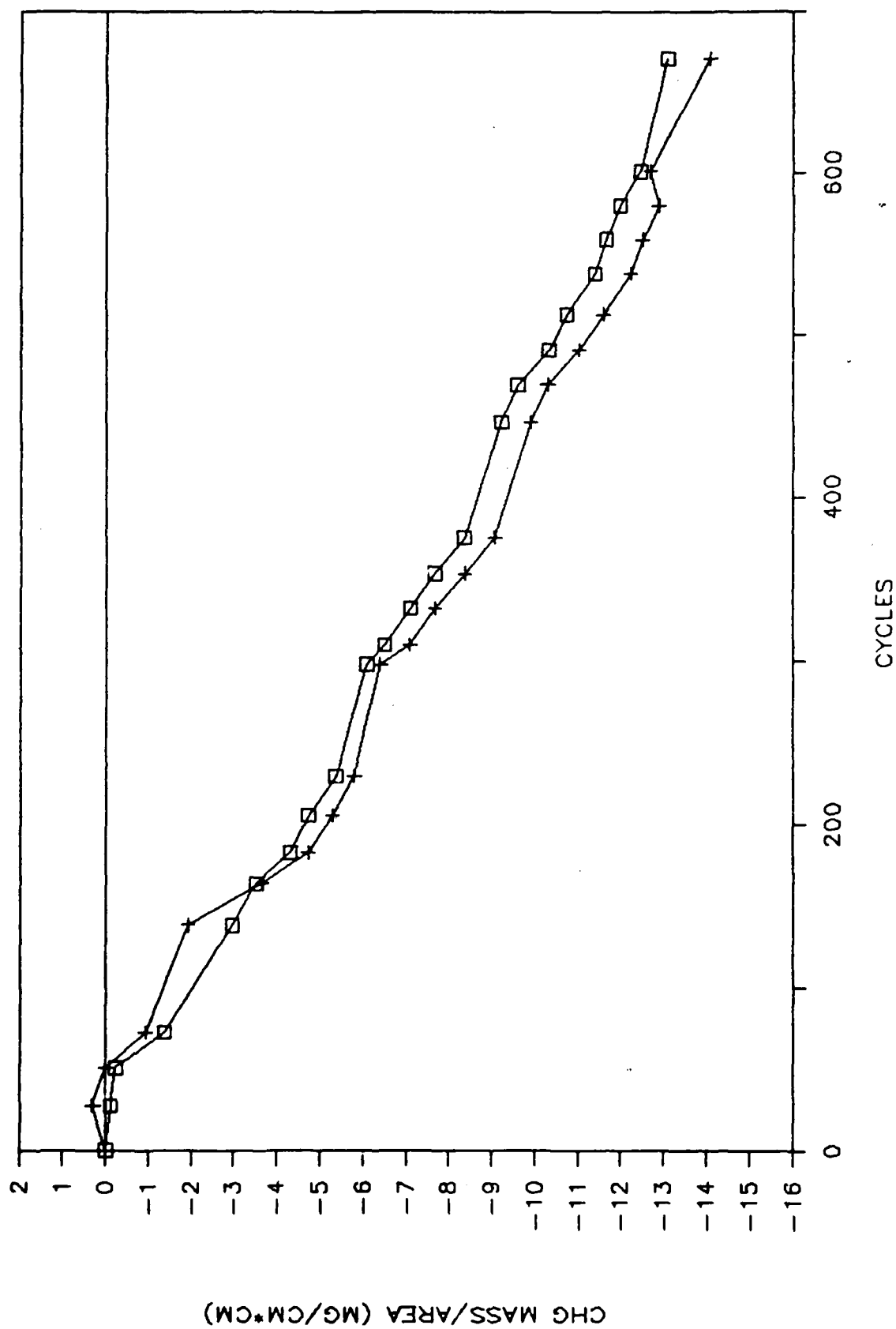


Figure 21 1180°C cyclic oxidation test results for Ni-30 wt. % Al-1 wt. % Cr.

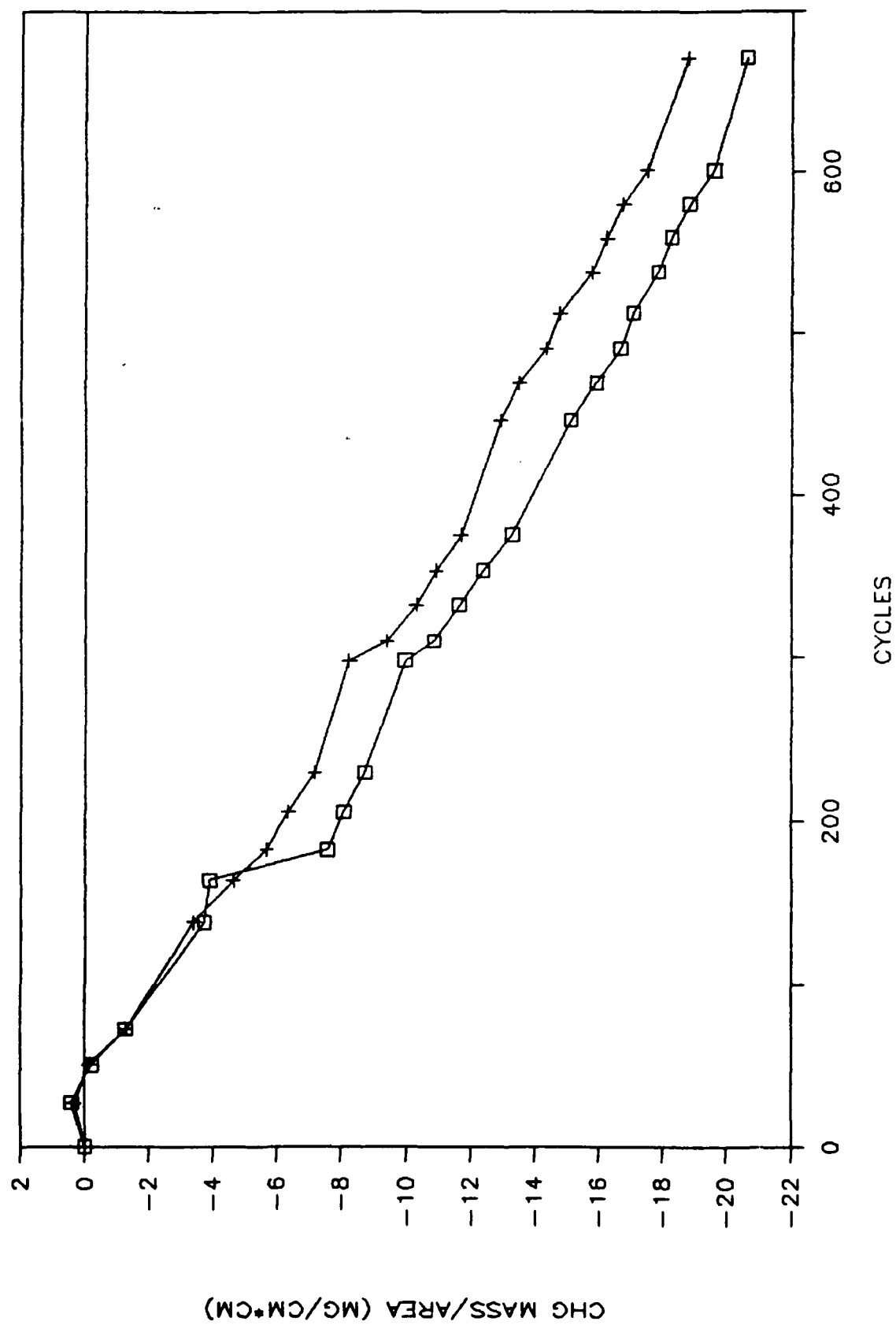


Figure 22 1180°C cyclic oxidation test results for Ni-30 wt. %Al-3 wt. % Cr.

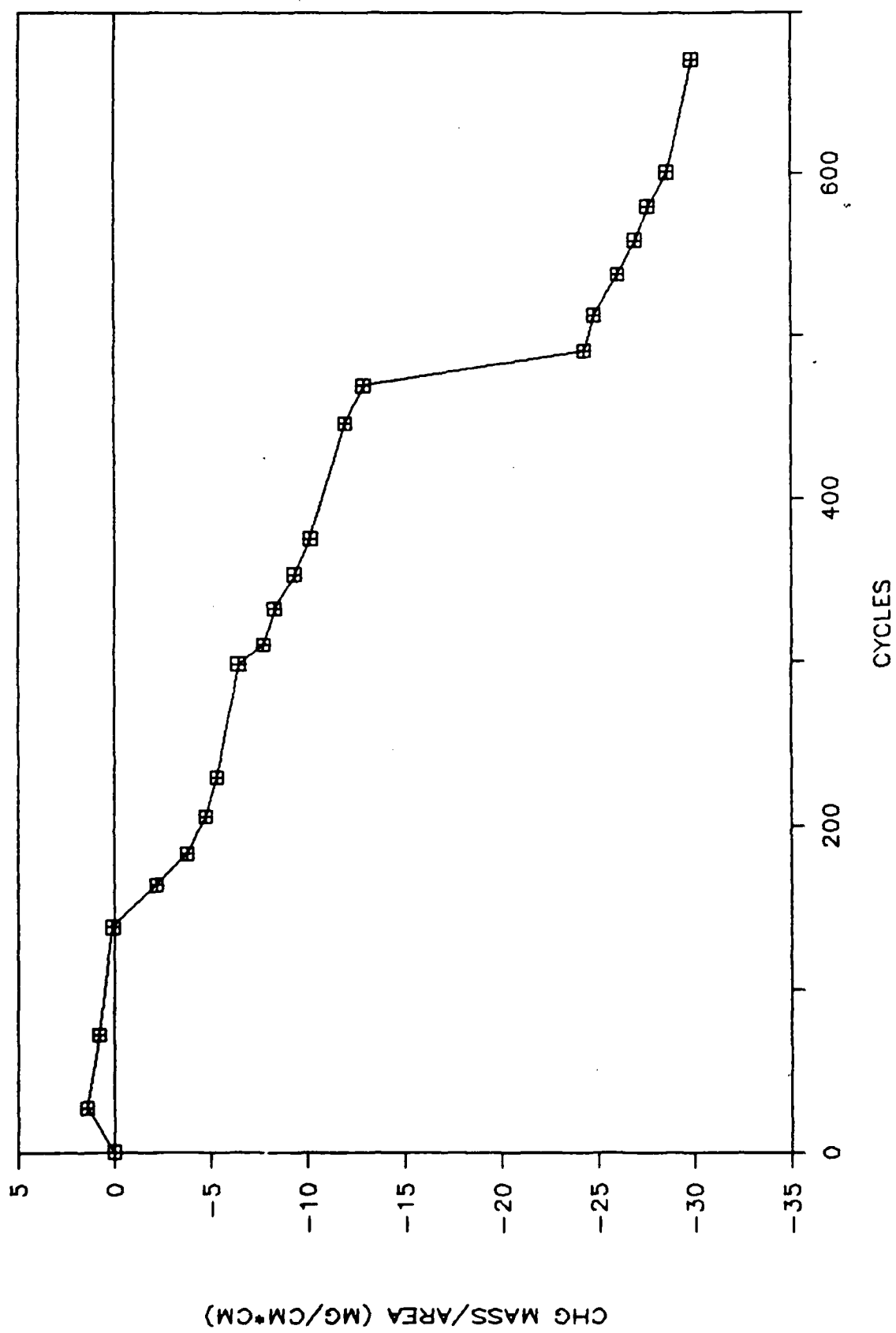


Figure 23 1180°C cyclic oxidation test results for Ni-30 wt. % Al-5 wt. % Cr.

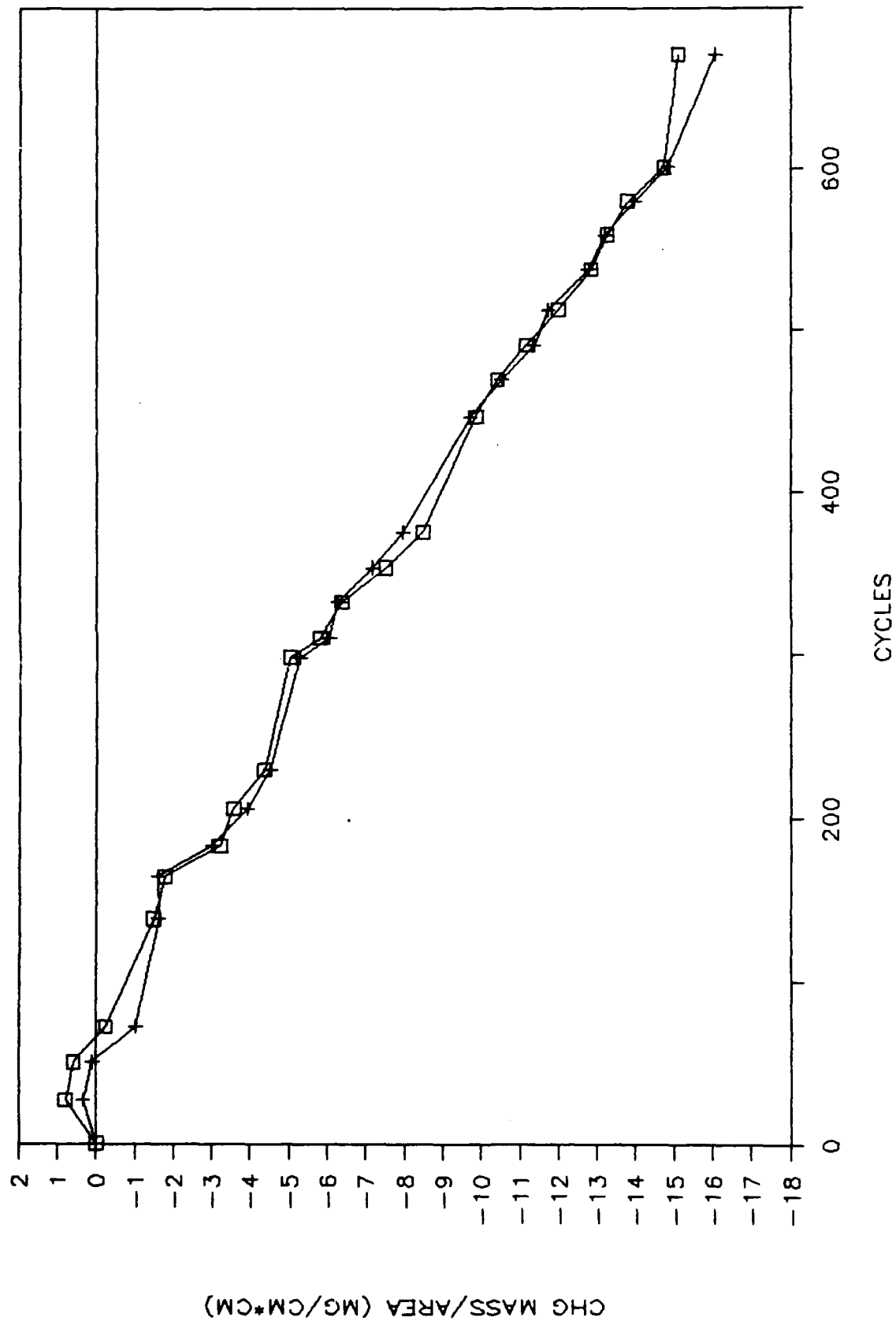


Figure 24 1180°C cyclic oxidation test results for Ni-30 wt. % Cr-7 wt. % Cr

## ONR BASIC DISTRIBUTION LIST

<u>Organization</u>	<u>Copies</u>	<u>Organization</u>	<u>Copies</u>
Defense Documentation Center Cameron Station Alexandria VA 22314	12	Naval Air Propulsion Test Center Trenton NJ 08628 ATTN: Library	1
Office of Naval Research Department of the Navy 800 N. Quincy Street Arlington VA 22217 ATTN: Code 431	3	Naval Construction Battalion Civil Engineering Laboratory Port Hueneme CA 93043 ATTN: Materials Division	1
Naval Research Laboratory Washington DC 20375 ATTN: Codes 6000 6300 2627	1 1 1	Naval Electronics Laboratory San Diego CA 92152 ATTN: Electronic Materials Sciences Division	   1
Naval Air Development Center Code 606 Warminster PA 18974 ATTN: Dr. J. Deluccia	1	Naval Missile Center Materials Consultant Code 3312-1 Point Mugu CA 92041	   1
Commanding Officer Naval Surface Weapons Center White Oak Laboratory Silver Spring MD 20910 ATTN: Library	1	Commander David W. Taylor Naval Ship Research and Development Center Bethesda MD 20084 ATTN: Code 012.5	   1 1
Naval Oceans Systems Center San Diego CA 92132 ATTN: Library	1	Naval Underwater System Center Newport RI 02840 ATTN: Library	  1
Naval Postgraduate School Monterey CA 93940 ATTN: Mechanical Engineering Department	1	Naval Weapons Center China Lake CA 93555 ATTN: Library	  1
Naval Air Systems Command Washington DC 20360 ATTN: Code 310A 5304B	1 1	NASA Lewis Research Center 21000 Brookpark Rd. Cleveland OH 44135 ATTN: Library	    1

## ONR BASIC DISTRIBUTION LIST (Continued)

<u>Organization</u>	<u>Copies</u>	<u>Organization</u>	<u>Copies</u>
Naval Sea System Command Washington DC 20362 ATTN: Code 05R	1	National Bureau of Standards Washington DC 20234 ATTN: Metals Science and Standards Standards Division	1
		Ceramic Glass and Solid State Science Division	1
		Fracture and Deformation Division	1
Naval Facilities Engineering Command Alexandria VA 22331 ATTN: Code 03	1	Defense Metals and Ceramics Information Center Battelle Memorial Institute 505 King Avenue Columbus OH 43201	1
Scientific Advisor Commandant of the Marine Corps Washington DC 20380 ATTN: Code AX	1	Metals and Ceramics Division Oak Ridge National Laboratory P.O. Box X Oak Ridge TN 37380	1
Army Research Office P.O. Box 12211 Triangle Park NC 27709 ATTN: Metallurgy and Ceramics Program	1	Los Alamos Scientific Laboratory P.O. Box 1663 Los Alamos NM 87544 ATTN: Report Librarian	1
Army Materials and Mechanics Research Center Watertown MA 02172 ATTN: Research Programs Office	1	Argonne National Laboratory Metallurgy Division P.O. Box 229 Lemont IL 60439	1
Air Force Office of Scientific Research/NE Building 410 Bolling Air Force Base Washington DC 20332 ATTN: Electronics and Materials Science Directorate	1	Brookhaven National Laboratory Technical Information Division Upton, Long Island NY 11973 ATTN: Research Library	1

## ONR BASIC DISTRIBUTION LIST (Continued)

<u>Organization</u>	<u>Copies</u>	<u>Organization</u>	<u>Copies</u>
NASA Headquarters		Library	
Washington DC 20546		Building 50, Room 134	
ATTN: Code RRM	1	Lawrence Radiation Laboratory	
		Berkeley CA	1